

T-3232

THE APPLICATION OF AN ION-INTERACTION MODEL TO  
SOLUBILITIES OF SOME ALKALINE-EARTH CARBONATES,  
THO<sub>2</sub> AND UO<sub>2</sub> IN BRINES

ARTHUR LAKES LIBRARY  
COLORADO SCHOOL of MINES  
GOLDEN, COLORADO 80401

by

James F. Ranville

ProQuest Number: 10782816

All rights reserved

INFORMATION TO ALL USERS

The quality of this reproduction is dependent upon the quality of the copy submitted.

In the unlikely event that the author did not send a complete manuscript and there are missing pages, these will be noted. Also, if material had to be removed, a note will indicate the deletion.



ProQuest 10782816

Published by ProQuest LLC (2018). Copyright of the Dissertation is held by the Author.

All rights reserved.

This work is protected against unauthorized copying under Title 17, United States Code  
Microform Edition © ProQuest LLC.

ProQuest LLC.  
789 East Eisenhower Parkway  
P.O. Box 1346  
Ann Arbor, MI 48106 – 1346

T-3232

A thesis submitted to the Faculty and Board of Trustees  
of the Colorado School of Mines in partial fulfillment of  
the requirements for the degree of Master of Science  
(Geochemistry).

Golden, Colorado

Date April 27, 1988

Signed: James F. Ranville  
James F. Ranville

Approved: Donald Langmuir  
Dr. Donald Langmuir  
Thesis Advisor

Golden, Colorado

Date 27 April 1988

George Kennedy  
Dr. George Kennedy, Head  
Department of Chemistry/  
Geochemistry

ABSTRACT

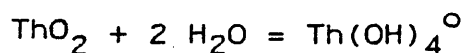
The goal of this research was to further the understanding of geochemical controls on radionuclide mobility in brines. To achieve this, the effect of ionic strength on the activities of carbonate, Th(IV), and U(IV) aquo-species was investigated both empirically and theoretically using the Pitzer ion-interaction model to compute ion activity coefficients.

The solubility of nesquehonite ( $\text{MgCO}_3 \cdot 3\text{H}_2\text{O}$ ) in NaCl brines between 15 and 35°C was measured to evaluate the Mg-HCO<sub>3</sub> and Mg-CO<sub>3</sub> Pitzer ion-interaction parameters. The Pitzer-computed  $\log K_{sp}$  in NaCl brines, over an ionic strength range of 0.4 to 5.5 molal, equaled  $-5.58 \pm 0.03$  at 25°C. From the measured solubility of nesquehonite in pure water at 25°C, and using an ion association model approach to compute ion activities,  $\log K_{sp}$  equaled -5.44. This compares with  $\log K_{sp} = -5.53$  computed with the same approach from nesquehonite solubility measurements reported by Langmuir (1965).

Based upon these results, and recent published evaluations of Pitzer parameters, a set of such parameters was adapted for ion-interaction modeling of mineral saturation in brines from the Palo Duro basin, Texas. Seventeen brines were collected for modeling. The

alkaline-earth sulfate minerals, gypsum, celestite and barite were at or near saturation in all the brines. Radium sulfate ( $\text{RaSO}_4$ ) was undersaturated. Radium concentrations may be limited by incorporation into a solid solution with barite ( $\text{BaSO}_4$ ). To model carbonate mineral saturation and lacking alkalinity data, it was necessary to assume calcite saturation. With this assumption, dolomite was the only other carbonate at saturation in the Palo Duro brines. A near-constant degree of undersaturation of strontianite ( $\text{SrCO}_3$ ) may indicate solid solution of  $\text{Sr}^{2+}$  in calcite. The overall implications are that sulfate minerals, but not carbonates, limit maximum concentrations of radionuclides such as  $^{90}\text{Sr}$  and Ra in the Palo Duro brines.

In the second part of the study the solubility of  $\text{ThO}_2$  was measured in NaCl brines at  $35^\circ\text{C}$ . The experimental results led to  $\log K = -9.58 \pm 0.4$  for the reaction



In ion interaction calculations of uranium species activities,  $\text{Th}^{4+}$ ,  $\text{La}^{3+}$ ,  $\text{Ba}^{2+}$  and  $\text{Cs}^+$  interaction parameters were used to model the activities of the U(IV) hydroxide complexes of the same charge. Ion-interaction modeling of four Palo Duro brines showed near saturation with respect to

T-3232

crystalline  $\text{ThO}_2$  in the Sawyer well, zone 4, Mansfield well, zone 1 and Sawyer well, zone 5.  $\text{ThO}_2$  was somewhat undersaturated in the Mansfield well, zone 2. Uranium concentrations were highly supersaturated with respect to crystalline  $\text{UO}_2$  in all four brines. This result may indicate that uranium is present in the oxidized U(VI) state as uranyl-carbonate complexes.

## TABLE OF CONTENTS

ABSTRACT .....	iii
LIST OF FIGURES .....	vii
LIST OF TABLES .....	viii
ACKNOWLEDGMENTS .....	x
INTRODUCTION .....	1
THERMODYNAMICS AND CHEMICAL MODELING OF GROUNDWATERS .....	3
DETERMINATION OF ACTIVITY COEFFICIENTS .....	4
CARBONATE SOLUBILITY STUDY	
Introduction .....	9
Carbonate Pitzer interaction parameters .....	10
Magnesium carbonate phase relations .....	19
NESQUEHONITE SOLUBILITY EXPERIMENTS	
Experimental .....	22
Results .....	27
Conclusions .....	38
PALO DURO BASIN BRINES STUDY	
Geology and hydrology .....	40
Chemistry of the Palo Duro brines .....	45
Temperature and pressure effects .....	51
Mineral saturation in the Palo Duro brines .....	56
Conclusions .....	63

ThO<sub>2</sub> AND UO<sub>2</sub> SOLUBILITY STUDY

Introduction .....	65
Previous ThO <sub>2</sub> Work .....	66
Modeling thorium complexes in brines .....	68
Experimental .....	79
Results .....	80
Effect of pH, I, and T on ThO <sub>2</sub> solubility .....	86
Effect of pH, I, and T on UO <sub>2</sub> solubility .....	88
ThO <sub>2</sub> and UO <sub>2</sub> solubility in the Palo Duro brines .....	92
REFERENCES CITED .....	102
APPENDIX I .....	109

## LIST OF FIGURES

<u>Figure</u>	<u>Page</u>
1	Stability diagram for the system Mg-CO <sub>3</sub> -OH-H <sub>2</sub> O at 25°C and 1 atm. total pressure .....23
2	The Palo Duro basin and the locations of the sample wells .....41
3	Distribution of Th <sup>4+</sup> and Th-aquo complexes as a function of pH in 0.1 molal NaCl at 25°C .....75
4	Distribution of Th <sup>4+</sup> and Th-aquo complexes as a function of pH in 0.5 molal NaCl at 25°C .....76
5	Distribution of Th <sup>4+</sup> and Th-aquo complexes as a function of pH in 1.0 molal NaCl at 25°C .....77
6	Distribution of Th <sup>4+</sup> and Th-aquo complexes as a function of pH in 4.0 molal NaCl at 25°C .....78
7	Distribution of U <sup>4+</sup> and U-aquo complexes as a function of pH in 0.1 molal NaCl at 25°C .....90
8	Distribution of U <sup>4+</sup> and U-aquo complexes as a function of pH in 0.5 molal NaCl at 25°C .....91
9	Distribution of U <sup>4+</sup> and U-aquo complexes as a function of pH in 1.0 molal NaCl at 25°C .....92
10	Distribution of U <sup>4+</sup> and U-aquo complexes as a function of pH in 4.0 molal NaCl at 25°C .....93
11	Effect of pH, ionic strength and temperature on the solubility of UO <sub>2</sub> .....95

## LIST OF TABLES

<u>Table</u>	<u>Page</u>
1 Second and third virial coefficients for the system Na-K-Ca-Mg-Cl-SO <sub>4</sub> -HCO <sub>3</sub> -CO <sub>3</sub> -H <sub>2</sub> O at 25°C .....	11
2 Pitzer $\phi$ and $\psi$ parameters for the carbonate system at 25°C .....	13
3 Pitzer computed log K <sub>sp</sub> 's for calcite at 25°C .....	16
4 Solubility products for minerals in the system Mg-HCO <sub>3</sub> -CO <sub>3</sub> -H <sub>2</sub> O at 25°C .....	20
5 Results of nesquehonite solubility experiments at 15°C and P(CO <sub>2</sub> ) = 0.78 atm. ....	28
6 Results of nesquehonite solubility experiments at 25°C and P(CO <sub>2</sub> ) = 0.78 atm. ....	29
7 Results of nesquehonite solubility experiments at 35°C and P(CO <sub>2</sub> ) = 0.78 atm. ....	30
8 Values of log K <sub>sp</sub> for nesquehonite at 15, 25 and 35°C .....	34
9 Pitzer model computed activities of Mg <sup>2+</sup> , CO <sub>3</sub> <sup>2-</sup> and H <sub>2</sub> O and log IAP of nesquehonite for the 15°C solubility run .....	35
10 Pitzer model computed activities of Mg <sup>2+</sup> , CO <sub>3</sub> <sup>2-</sup> and H <sub>2</sub> O and log IAP of nesquehonite for the 25°C solubility run .....	36
11 Pitzer model computed activities of Mg <sup>2+</sup> , CO <sub>3</sub> <sup>2-</sup> and H <sub>2</sub> O and log IAP of nesquehonite for the 35°C solubility run .....	37
12 A brief description of the major lithologic components of the Palo Duro cores .....	43
13 DOE wells in the Palo Duro basin, Texas, and their units, major lithologies, and depths sampled .....	46
14 Temperatures and pressures in the Palo Duro sampling intervals .....	47

15	Molal concentrations of major chemical species in the Palo Duro brines .....	49
16	Molal activities of the major species in the Palo Duro brines computed using the Pitzer equations .....	57
17	Saturation indices for selected minerals in the Palo Duro brines computed using Pitzer equations ...	59
18	Carbonate mineral saturation indices in the Palo Duro brines computed using Pitzer equations and assuming calcite saturation .....	62
19	Cumulative formation constants at 25°C for mononuclear Th(IV)-hydroxy complexes written in the proton form .....	67
20	Thermodynamic data for ThO <sub>2</sub> and thorium aqueous species at 25°C and 1 atm. pressure .....	69
21	Pitzer ion-interaction parameters for the thorium species in NaCl solutions at 25°C .....	72
22	Model computed activity coefficients of thorium species in NaCl media at 25°C using analogous species .....	73
23	Molal concentrations of <sup>232</sup> Th and final pH's in NaCl solutions at 35°C .....	81
24	Experimentally determined equilibrium constants (-log K <sub>eq</sub> values) for reaction (32) in NaCl solutions at 35°C .....	84
25	Effect of pH, ionic strength and temperature on the solubility of ThO <sub>2</sub> in NaCl media .....	86
26	Cumulative formation constants at 25°C for mononuclear U(IV)-hydroxy complexes written in the proton form .....	89
27	Molal concentrations of thorium and uranium in some Palo Duro brines .....	96
28	Predicted and measured -log molal solubilities of ThO <sub>2</sub> and UO <sub>2</sub> in some Palo Duro brines .....	98

ACKNOWLEDGMENTS

I would like to acknowledge Battelle, Columbus for funding this research under CSM contract 082-747. I would like to thank Dr. Donald Langmuir his helpful advice on this thesis and for gaining some measure of understanding of aqueous geochemistry. I wish also to thank the other members of my committee for their useful suggestions and support. Finally a special thank you to my parents and my friends at CSM whose support is greatly appreciated. I wish to also acknowledge Dan Melchior who was of much help in the early stages of this work and also Ron Schmiermund who wrote the initial version of the IBM-PC speciation program.

## INTRODUCTION

The development of nuclear power has brought many problems, including the generation of large quantities of high-level radioactive wastes. The nuclear power industry thus needs an acceptable means for disposal of such wastes. A major difficulty lies in the hazardous nature of these materials which contain highly radioactive elements as well as long-lived radionuclides. A possible solution is to isolate the wastes in deep, geologically situated repositories, out of contact with the surficial environment and human contact. The Nuclear Waste Policy Act of 1982 requires the Department of Energy to 'select and characterize the candidate sites selected for the construction and operation of a geological repository for the disposal of high level nuclear wastes'. DOE is further charged in 10 CFR 60.113 to assure "substantially complete containment (of wastes) within the waste package of 300 to 1000 years and controlled release rates from the engineered barrier system for 10,000 years or one part in  $10^5$  year of the inventory of radionuclides present in defined quantities 100 years after permant closure." Until recently (December 1987) three geologic locales were under consideration by the Department of Energy for a waste repository. These

included: the basalts of eastern Washington state; tuffs within the Nevada test site; and bedded salt formations of the Palo Duro basin in the Texas panhandle. This study is directed towards the bedded salts of the Palo Duro basin. Presently only the Nevada test site is under consideration as the primary repository site. The bedded salts may be reconsidered should the Nevada test site prove to be either scientifically or politically unsuitable.

To safely dispose of radioactive wastes in deep geological formations all aspects of this process and its consequences must be fully understood. One of the most important areas of research is the study of the chemical and hydrologic properties of ground waters associated with these sites and their proposed wastes. If a breach of the waste package should occur, it is these ground waters that would transport hazardous radionuclides toward surface environments. A goal of this research was to obtain information on the Palo Duro brines, related to their chemical properties which might influence the transport of radionuclides. In particular, the importance of the carbonate system was studied, in that uranyl carbonate complexing can greatly increase the solubility and mobility of radioactive uranium from  $UO_2$  dissolution.

THERMODYNAMICS AND CHEMICAL MODELING  
OF GROUNDWATERS

A standard approach in aqueous geochemistry is to apply thermodynamic principles to the interpretation of geochemical data on both ground waters and associated mineral phases. Either empirical equilibrium constants for minerals are used, or the Gibbs free energy, enthalpy, and entropy are employed to compute these mineral solubilities as a function of temperature. This approach then computes the relative saturation state of the ground water with respect to the mineral phases with which it is in contact. The mineral saturation calculation is facilitated by computer models which rapidly solve the equilibria involved. There are numerous such chemical equilibrium models available (cf. Nordstrom and Ball, 1984).

In most of these models activity coefficients ( $\gamma$ ) for ionic species are computed using the Debye-Huckel or Davies equations (Nordstrom and Munoz, 1986). These approaches are only accurate for relatively dilute waters, with ionic strengths well below that of seawater ( $I = 0.7m$ ). A major difficulty in applying equilibrium constants to solubility calculations in waters of high salinity is in obtaining accurate  $\gamma$  values as a function of ionic strength.

## DETERMINATION OF ACTIVITY COEFFICIENTS

As previously stated, to apply an equilibrium constant to a real solution, total measured concentrations of chemical species must be converted to activities through the use of activity coefficients. Much work has been done to obtain expressions which relate  $\gamma$  values to the concentrations of the various species in solution. The first approach, proposed in 1922 by Bronsted, states that for a 1:1 electrolyte the activity coefficient can be expressed as

$$\ln \gamma = -3 \alpha m^{1/2} - 2 \beta m \quad (1)$$

where  $\alpha$  depends on the charge of the ion and the nature of the solvent while  $\beta$  is specific to each electrolyte (cf. Pitzer, 1979). This model was followed by the more elegant and general model of Debye and Hückel (1923) which is still the standard means of calculating activity coefficients in dilute solutions. This approach, which accounts for long range electrostatic interactions between ions, is most useful in the form of the extended Debye-Hückel equation

$$\log \gamma = \frac{-A z^2 (I)^{1/2}}{1 + Ba(I)^{1/2}} \quad (2)$$

where A and B are constants which are a function of temperature and the dielectric constant of water, z is the charge on the ion, a is the hydrated ion size parameter in Angstroms and I is the molal or molar ionic strength. The values of A and B differ if molal or molar units are used. This equation accurately predicts the activity coefficients of ions in solutions of low ionic strength ( $I < 0.1m$ ). However, at moderate to high ionic strength ( $I > 0.5m$ ), measured values of  $\gamma$  begin to increase, whereas Debye-Hückel theory predicts continuously decreasing  $\gamma$  values as ionic strength increases. Several models add positive terms to the Debye-Hückel equation to increase predicted  $\gamma$  values. The most familiar of these is the Davies equation (cf. Nordstrom and Munoz, 1986)

$$\log \gamma = -Az^2 \left( \frac{(I)^{1/2}}{1 + (I)^{1/2}} \right) + 0.2(I) \quad (3)$$

which is accurate to approximately  $I = 0.5$  for 1:1 electrolytes. Guggenheim (cf. Pitzer, 1979) used principles from Bronsted and Debye and Hückel to develop his equation:

$$\ln \gamma = -A \frac{z^2(I)^{1/2}}{1+(I)^{1/2}} + \frac{(2v_+v_-)(2\beta)m}{v_+v_-} \quad (4)$$

where  $\beta$  is an ion interaction constant,  $v_+$  is the number of cations and  $v_-$  the number anions in the neutral salt, and the other terms are as previously defined.

An approach using a simplified Guggenheim equation coupled with the mean salt method proposed by Truesdell and Jones (1974) has been successful for single electrolyte solutions up to  $I=6m$ . Their equation is:

$$\log \gamma = \frac{-Az^2(I)^{1/2}}{1+Ba(I)^{1/2}} + bI \quad (5)$$

where  $a$  and  $b$  are constants for individual ions. This approach is less successful for mixed-electrolyte solutions.

A recent comprehensive approach to complex, high ionic strength solutions has been developed by Kenneth Pitzer and his colleagues, and is commonly called the ion-interaction approach (cf. Pitzer, 1977). This semi-empirical model was developed in part from statistical mechanics, which is used to obtain thermodynamic functions from the relationship between inter-ionic potentials and radial distribution

functions (Pitzer, 1973). The approach accounts for long-range electrostatic effects, as in the Debye-Hückel equation, but also for short-range interactions between ions that only occur in concentrated solutions. These include repulsive forces between two ions of like sign and interactions which involve three ions, which were ignored in previous approaches. The general form of Pitzer equations for calculating activity coefficients is given in Appendix I. The Pitzer equations are theoretically capable of modelling complex electrolyte mixtures containing as many different ions as desired, so long as their interaction parameters are known.

Several workers have incorporated the Pitzer equations into geochemical computer codes, the most recent and complete being that of Harvie et al. (1984). This program contains Pitzer ion-interaction parameters for the system Na-K-Ca-Mg-Cl-SO<sub>4</sub>-HCO<sub>3</sub>-CO<sub>3</sub>-H<sub>2</sub>O-CO<sub>2</sub> and has been successful in modeling experimental data in seawater and electrolyte solutions up to 20m ionic strength. Other workers have used Pitzer's equations to successfully model sulfate mineral equilibria (Rogers, 1981; Langmuir and Melchior, 1985; Reardon and Armstrong, 1987). Langmuir and Melchior considered five of the seventeen Palo Duro basin brines considered herein. Bassett and Bentley (1982) also employed

Pitzer equations to model carbonate equilibria in the Palo Duro and Dalhart basins. However, they employed a less complete set of Pitzer carbonate interaction parameters and no consideration of temperature effects on the coefficients was given. Monnin and Schott (1984) examined the saturation state of sodium carbonate, trona, in waters of Lake Magadi, Kenya, using Pitzer equations. Millero (1983) estimated the effective acidity constants of a number of acids in seawater using Pitzer equations.

A goal of my research was to use the Pitzer equations to model the geochemistry of carbonate minerals in some Palo Duro basin brines. The first step in this effort was to perform laboratory experiments on carbonate solubility in various electrolyte solutions in order to evaluate the carbonate interaction parameters. The ground water chemistry data was then modeled using the Pitzer equations to obtain solution species activities. The results were used to compute the saturation indices for various minerals. Of special interest were the saturation states of the sulfate and carbonate minerals which might limit radionuclide mobility in the brine aquifers.

The effect of ionic strength on the solubility of  $\text{ThO}_2$ , thorianite, was measured and the data used to determine activity coefficients for thorium aquo-species. These

results were used to determine if  $\text{ThO}_2$  was at saturation in Palo Duro ground waters. The results of the  $\text{ThO}_2$  experiments were used by analogy to model  $\text{UO}_2$  solubility in the same reduced brines.

## CARBONATE SOLUBILITY STUDY

### Introduction

Carbonate minerals such as calcite and dolomite, limit maximum concentrations of Ca and Mg in many ground waters. Calcite can incorporate Ba, Sr and Ra in solid solution and thereby exercise control over the aqueous concentrations of these elements (cf. Sverjensky, 1984). This may have importance in determining the maximum aqueous concentration of  $^{90}\text{Sr}$  (cf. Mucci and Morse, 1983). Also  $\text{HCO}_3^-$  and  $\text{CO}_3^{2-}$  ions form complexes with many cations, thereby affecting the solution behavior of many important chemical species and increasing their solubilities. Especially important is complexing between  $\text{UO}_2^{2+}$  and  $\text{CO}_3^{2-}$  (Langmuir, 1978). For these reasons it is necessary to obtain information on the relationships between activity coefficients of the aqueous carbonate species and ionic strength.

An objective of this research was to determine the activity coefficients of aqueous species in the calcium and

magnesium carbonate systems using the Pitzer ion-interaction model. Pitzer coefficients are available for these systems (Harvie, 1981) but are not extensive. In order to evaluate the reliability of the magnesium and carbonate parameters, the effect of ionic strengths up to 5.5m on the solubility product ( $K_{sp}$ ) of nesquehonite was investigated. The experiments were performed under a  $CO_2$  saturated atmosphere, under which conditions nesquehonite is the stable mineral phase (see Figure 1). These conditions were chosen to better control the carbonate system and to increase carbonate mineral solubility. Solubility results were modeled using the Pitzer ion-interaction equations to obtain experimental nesquehonite  $K_{sp}$  values as a function of ionic strength. The results were compared to  $K_{sp}$  values from the literature. Published calcite solubilities measured in brines were similarly evaluated.

#### Carbonate interaction parameters

Ion-interaction parameters for the carbonate system have been developed by a number of workers. The parameters for the system Na-K-Ca-Mg-Cl- $SO_4$ - $HCO_3$ - $CO_3$ - $H_2O$  as compiled by Harvie et al. (1984) and Weare (1987) are given in Tables 1 and 2. The Na- $HCO_3$  (Pitzer and Peiper, 1980) and Na- $CO_3$  (Peiper and Pitzer, 1982) parameters were obtained from

Table 1. Second and third virial coefficients for the system Na-K-Ca-Mg-H-Cl-SO<sub>4</sub>-CO<sub>3</sub>-H<sub>2</sub>O at 25°C from Harvie et al. (1984).

Species	$\beta^0$	$\beta^1$	$\beta^2$	$C^0$
NaCl	0.0765	0.2644	-	0.00127
Na <sub>2</sub> SO <sub>4</sub>	0.01958	1.113	-	0.00497
NaHCO <sub>3</sub>	0.0277	0.0411	-	-
Na <sub>2</sub> CO <sub>3</sub>	0.0399	1.389	-	0.0044
NaOH	0.0864	0.253	-	0.0044
KCl	0.04835	0.2122	-	-0.00084
K <sub>2</sub> SO <sub>4</sub>	0.04995	0.7793	-	-
KHCO <sub>3</sub>	0.0296	-0.013	-	-0.008
K <sub>2</sub> CO <sub>3</sub>	0.1488	1.43	-	-0.0015
KOH	0.1298	0.320	-	0.0041
CaCl <sub>2</sub>	0.3159	1.614	-	-0.00034
CaSO <sub>4</sub>	0.20	3.1973	-54.24	-
Ca(HCO <sub>3</sub> ) <sub>2</sub>	0.4	2.977	-	-
CaCO <sub>3</sub>	0	0	0	0
Ca(OH) <sub>2</sub>	-0.1747	-0.2303	-5.72	-
MgCl <sub>2</sub>	0.35235	1.6815	-	0.00519
MgSO <sub>4</sub>	0.2210	3.343	-37.23	0.025
Mg(HCO <sub>3</sub> ) <sub>2</sub>	0.329	0.6072	-	-
MgCO <sub>3</sub>	0	0	0	0

(continued)

Table 1. (continued).

Species	$\beta^0$	$\beta^1$	$\beta^2$	$C^0$
$Mg(OH)_2$	-	-	-	-
HCl	0.1775	0.2945	-	0.0008
$H_2SO_4$	0.298	-	-	0.0438
$H_2CO_3$	-	-	-	-

Table 2. Pitzer  $\phi$  and  $\Psi$  parameters for the carbonate system at 25°C from Harvie et al. (1984).

i j	$\phi_{ij}$	$\Psi_{ij}Cl$	$\Psi_{ij}SO_4$	$\Psi_{ij}HCO_3$	$\Psi_{ij}CO_3$
Na K	-0.012	-0.0018	-0.010	-0.003	0.003
Na Ca	0.07	-0.007	-0.055	-	-
Na Mg	0.07	-0.012	-0.015	-	-
Na H	0.036	-0.004	-	-	-
K Ca	0.032	-0.025	-	-	-
K Mg	0.0	-0.022	-0.048	-	-
K H	0.005	-0.011	0.197	-	-
Ca Mg	0.007	-0.012	0.024	-	-
Ca H	0.092	-0.015	-	-	-
Mg H	0.10	-0.011	-	-	-

(continued)

Table 2. (continued).

i	j	$\phi_{ij}$	$\psi_{ijNa}$	$\psi_{ijK}$	$\psi_{ijCa}$	$\psi_{ijMg}$
Cl	SO <sub>4</sub>	0.02	0.0014	-	-0.018	-0.004
Cl	OH	-0.050	-0.006	-0.006	-0.025	-
Cl	HCO <sub>3</sub>	0.03	-0.015	-	-	-0.096
Cl	CO <sub>3</sub>	-0.02	0.0085	0.004	-	-
SO <sub>4</sub>	OH	-0.013	-0.009	-0.050	-	-
SO <sub>4</sub>	HCO <sub>3</sub>	0.01	-0.005	-	-	-0.161
SO <sub>4</sub>	CO <sub>3</sub>	0.02	-0.005	-0.009	-	-
OH	HCO <sub>3</sub>	-	-	-	-	-
OH	CO <sub>3</sub>	0.10	-0.017	-0.01	-	-
HCO <sub>3</sub>	CO <sub>3</sub>	-0.04	0.002	0.012	-	-

electrochemical cell measurements. The Na-CO<sub>3</sub> parameters (Harvie, 1982) were also estimated from emf and isopiestic measurements. Remaining parameters for the Na-Cl-SO<sub>4</sub>-HCO<sub>3</sub>-CO<sub>3</sub>-H<sub>2</sub>O system were obtained by evaluating solubility measurements in common-ion systems (Harvie et al., 1984).

There is less data available for the corresponding K-Cl-SO<sub>4</sub>-HCO<sub>3</sub>-CO<sub>3</sub>-H<sub>2</sub>O system. Pitzer and Peiper (1982) estimated  $\beta^{1K,HCO_3}$  and Harvie (1981) estimated  $\beta^{1K,CO_3}$  from emf data. Higher-order parameters for this system were derived from solubility data (Harvie, 1981).

Harvie et al (1984) obtained interaction parameters for Ca-HCO<sub>3</sub> and Ca-CO<sub>3</sub> from the calcite solubility work of Shternina and Frolova (1952, 1962), Frear and Johnson (1929) and Cameron et al. (1907). The calcite solubility data in NaCl obtained from these workers covers an ionic strength range of 0.008 to 6.3 molal and a CO<sub>2</sub> pressure, P(CO<sub>2</sub>), range of 0.00033 to 0.97 bars. Their results were modeled using the interaction parameters from Harvie et al. (1984) to obtain values for the K<sub>sp</sub> of calcite as a function of ionic strength. Table 3 shows the relatively good agreement between the Pitzer-computed log K<sub>sp</sub>'s and the 25°C value of -8.48 obtained by Plummer and Busenberg (1982).

Millero et al. (1984) used existing Ca-HCO<sub>3</sub> and Ca-CO<sub>3</sub> parameters to explain the solubilities of calcite,

Table 3. Pitzer-computed  $\log -K_{sp}$ 's for calcite at 25°C from the solubility data of Shternina and Frolova (1952,1962)(column A) and Frear and Johnson(1929) (column B).

I(m)	A $-\log K_{sp}$	I(m)	B $-\log K_{sp}$
0.03	8.37	0.03	8.43
0.11	8.53	0.04	8.43
0.21	8.49	0.06	8.47
0.39	8.49	0.11	8.47
1.47	8.32	0.27	8.48
1.97	8.35	0.33	8.55
2.46	8.39	0.64	8.47
3.08	8.43	0.86	8.56
5.31	8.32	0.92	8.48
6.27	8.71	1.13	8.61
		1.20	8.49
mean	8.44 ± 0.12	mean	8.49 ± 0.06
		grand mean	8.47 ± 0.09

strontianite ( $\text{SrCO}_3$ ) and witherite ( $\text{BaCO}_3$ ) in NaCl solutions at atmospheric  $\text{CO}_2$  pressure ( $\log P(\text{CO}_2) = -3.5$  bars) and  $25^\circ\text{C}$ . He found the Pitzer-computed  $\log K_{\text{sp}}$  values for the respective minerals to be within  $\pm 0.02$ ,  $\pm 0.14$ , and  $\pm 0.26$  of the preferred thermodynamic values. From the above results, it was determined that interaction parameters for the  $\text{Ca-HCO}_3\text{-CO}_3\text{-H}_2\text{O}$  system were of sufficient accuracy to be used in this study.

The  $\text{Mg-HCO}_3\text{-CO}_3$  system has not been studied as extensively as the  $\text{Ca-HCO}_3\text{-CO}_3$  system. Harvie et al. (1984) obtained  $\text{Mg-HCO}_3$  and  $\text{Mg-CO}_3$  parameters from the solubility work of Mitchell (1923) and Kline (1929), the phase equilibria data of Tredafelov et al. (1981) and from estimates of apparent carbonate dissociation constants in seawater by Hansson (1973). Millero (1983) developed interaction parameters for  $\text{Mg-HCO}_3$  and  $\text{Mg-CO}_3$  in seawater ( $I = 0.7$ ) from the effect of presumed formation of  $\text{MgHCO}_3^+$  and  $\text{MgCO}_3^0$  on the apparent dissociation constants of  $\text{H}_2\text{CO}_3$  and  $\text{HCO}_3^-$ . However Millero's parameters are only applicable at the ionic strength of seawater. Due to the apparent uncertainty in the  $\text{Mg-HCO}_3$  and  $\text{Mg-CO}_3$  interaction parameters, particularly above  $I = 0.7\text{m}$  (cf. Harvie et al., 1984) a magnesium carbonate solubility study was undertaken.

A computer code containing the Pitzer equations was

obtained from Dr. Pamela Rogers. This code was modified to include a carbonate speciation subroutine. This subroutine allows computation of the concentrations and activities of  $\text{HCO}_3^-$  and  $\text{CO}_3^{2-}$ , given a number of different pairs of carbonate input parameters. The possible combinations used in this study were  $P(\text{CO}_2)$  and pH, pH and  $\text{mHCO}_3^-$ , and  $P(\text{CO}_2)$  and  $\text{mHCO}_3^-$ . The subroutine was written using the carbonate species temperature functions of  $K_h$ ,  $K_1$  and  $K_2$  given by Plummer and Busenberg (1982) which are:

$$K_h = 108.3865 + 0.01985076 T - 6919.53/T - 40.45154 \log T + 669365/T^2 \quad (6)$$

$$K_1 = -356.3094 - 0.06091964 T + 21834.37/T + 126.8339 \log T - 1684915/T^2 \quad (7)$$

$$K_2 = -107.8871 - 0.03252849 T + 5151.79/T + 38.92561 \log T - 563713.9/T^2 \quad (8)$$

where  $K_h = [\text{H}_2\text{CO}_3]/P(\text{CO}_2)$ ,  $K_1$  and  $K_2$  are first and second dissociation constants of carbonic acid, and  $T$  is in degrees Kelvin. This subroutine also corrects the input pH for liquid junction potentials using the Henderson equation (cf. Bates, 1973) and assuming a saturated KCl salt bridge as was

used in this study.

The sources of interaction parameters for the sulfate system have been summarized by Melchior (1984). Additionally the reader is referred to Harvie (1982) for a more complete discussion of the sources of Pitzer ion-interaction parameters.

### Magnesium carbonate phase relations

The Mg-HCO<sub>3</sub>-CO<sub>3</sub>-H<sub>2</sub>O system has been investigated by Langmuir (1965), Schott and Dandurand (1975) and Ming (1982). The minerals considered important by these authors at 25°C and 1 atm. total pressure are brucite (Mg(OH)<sub>2</sub>), hydromagnesite (4MgCO<sub>3</sub>·Mg(OH)<sub>2</sub>·4H<sub>2</sub>O), magnesite (MgCO<sub>3</sub>), and nesquehonite (MgCO<sub>3</sub>·3H<sub>2</sub>O). At temperatures below 10°C, lansfordite (MgCO<sub>3</sub>·5H<sub>2</sub>O) is also a stable carbonate phase. Two variables which determine the relative stabilities of these minerals are the activity of water ([H<sub>2</sub>O]) and P(CO<sub>2</sub>). The equilibrium constants necessary to compute a log [H<sub>2</sub>O], log P(CO<sub>2</sub>) stability diagram for these minerals (Figure 1) are given in Table 4.

The brucite-hydromagnesite phase boundary is computed from:

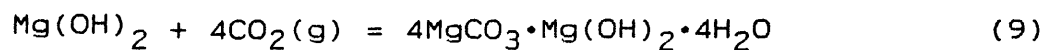


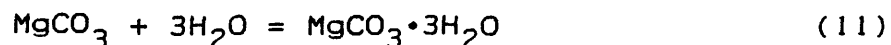
Table 4. Solubility products for minerals in the system  
Mg-HCO<sub>3</sub>-CO<sub>3</sub>-H<sub>2</sub>O at 25°C.

Mineral	K <sub>sp</sub>	Reference
Mg(OH) <sub>2</sub> (brucite)	-11.15	Smith and Martell (1976)
MgCO <sub>3</sub> (magnesite)	-5.10	Langmuir (1965)
MgCO <sub>3</sub> •3H <sub>2</sub> O	-5.59	Langmuir (1965)
(nesquehonite)	-5.42	Langmuir (1984)
	-5.42	Hostetler (1973)
	-5.07	Robie and Hemingway (1973)
	-5.60	NBS (1982)
MgCO <sub>3</sub> •5H <sub>2</sub> O	-5.29	Langmuir (1984)
(lansfordite)	-5.46	Langmuir (1965)
4MgCO <sub>3</sub> •Mg(OH) <sub>2</sub> •4H <sub>2</sub> O	-35.0	Langmuir (1984)
(hydromagnesite)		

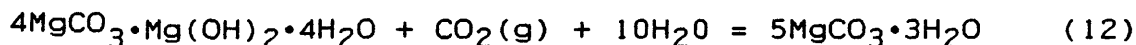
which when solved using equilibrium constants taken from Table 4 gives  $1/(P(\text{CO}_2))^4 = 10^{20.0}$ . This results in a boundary line independent of  $\log [\text{H}_2\text{O}]$  and  $\log P(\text{CO}_2) = -5.0$ . The magnesite-hydromagnesite boundary line is computed from



where  $P(\text{CO}_2)/[\text{H}_2\text{O}]^5 = 10^{0.648}$ . This expression results in a boundary line with a slope = +0.2. The magnesite-nesquehonite boundary line is computed from



where  $1/[\text{H}_2\text{O}]^3 = 10^{0.52}$  or  $10^{0.69}$  using the nesquehonite  $K_{\text{sp}}$  values of Hostetler (1973) and Langmuir (1984) or Langmuir (1965) respectively. The phase boundary between these two fields is independent of  $\log P(\text{CO}_2)$ , with  $\log [\text{H}_2\text{O}] = -0.173$  or  $-0.230$  using the values of Hostetler (1973) and Langmuir (1984) or Langmuir (1965), respectively. Finally, the hydromagnesite-nesquehonite boundary line is computed using the equation



where  $1/P(\text{CO}_2) \cdot [\text{H}_2\text{O}]^{10} = 10^{1.95}$  or  $10^{2.80}$ . The resulting stability boundary has a slope = 0.1. The resultant phase diagram for the  $\text{MgO}-\text{CO}_2-\text{H}_2\text{O}$  at  $25^\circ\text{C}$  is shown in Figure 1.

Experiments to determine the effect of ionic strength on nesquehonite solubility were performed using pure  $\text{CO}_2$  gas to increase the solubility of the carbonate phase. At the elevation of Golden, CO (1800 m), where the experiments were performed, the atmospheric pressure is approximately equal to 0.8 atm. The experiments were performed at ionic strengths between 0.2 and 5.5 molal NaCl. Under these conditions the activity of water ranges from 1.00 to 0.778. For these conditions the stable mineral phase is nesquehonite regardless of which  $K_{sp}$  is employed.

### Nesquehonite Solubility Experiments

#### Experimental

Nesquehonite was prepared from reagent grade basic magnesium carbonate,  $4\text{MgCO}_3 \cdot \text{Mg}(\text{OH})_2 \cdot 4\text{H}_2\text{O}$  (hydromagnesite), by first dissolving the solid in doubly-deionized water at  $25^\circ\text{C}$  under a water-saturated  $\text{CO}_2$  atmosphere of 0.78 atm. The solution was saturated with nesquehonite by adding additional hydromagnesite daily until no further dissolution of the solid was observed. The solution was then allowed to

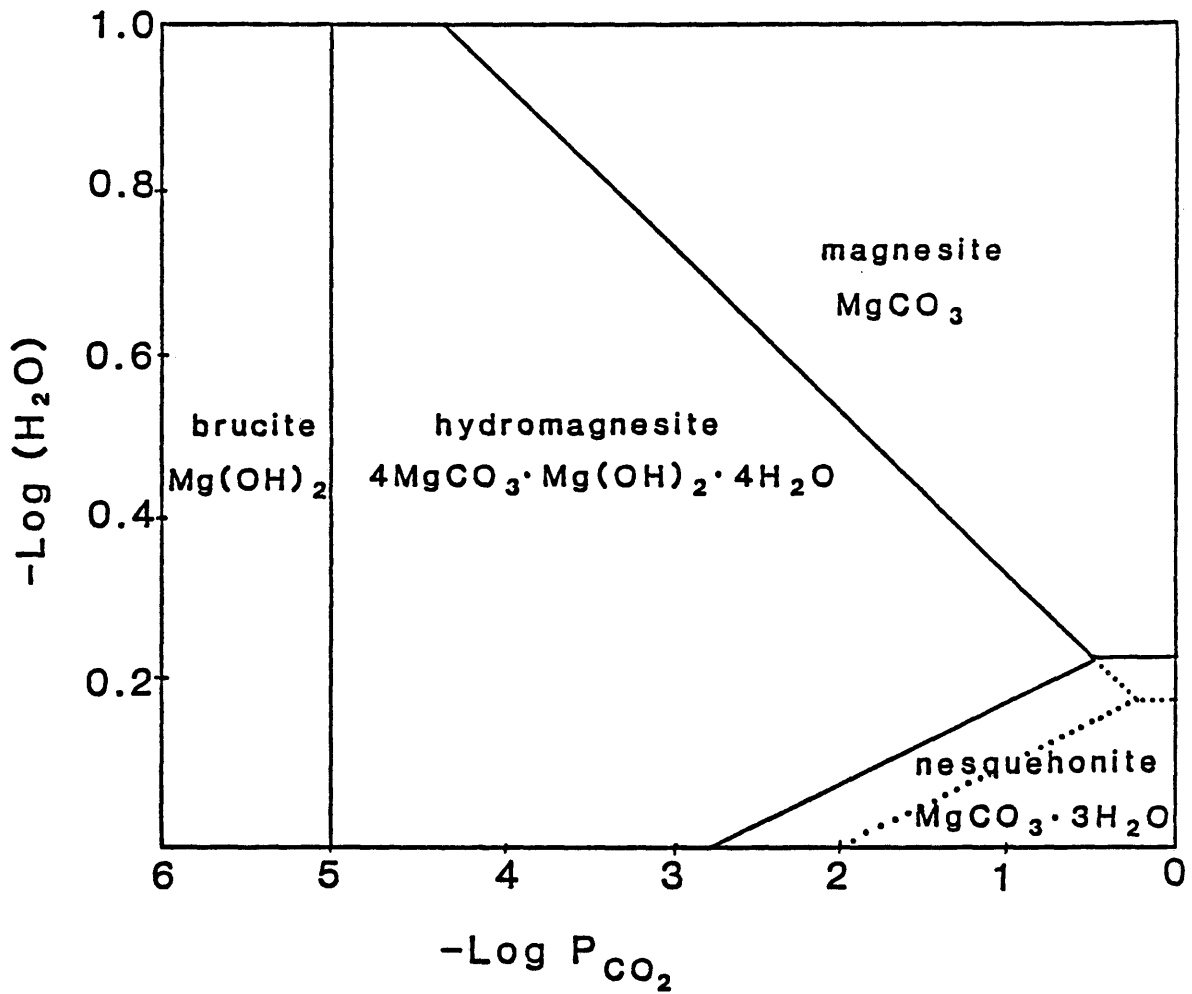


Figure 1. Stability diagram for the system Mg-CO<sub>3</sub>-OH-H<sub>2</sub>O at 25°C and 1 atm. total pressure (after Langmuir, 1965).

degas at 35°C for a few days as the nesquehonite precipitated out of solution. The solid was collected on Whatman ashless filter paper and stored in a sealed flask under a CO<sub>2</sub> atmosphere. Analysis of the solid by X-ray diffraction and comparison of d-spacings to literature values (Ming, 1982) verified it to be nesquehonite. The solid was also examined under an electron microscope which showed prismatic crystals with the expected pseudo-orthorombic habit (Ming, 1982).

Solutions of varying ionic strengths used in the solubility experiments were prepared from oven-dried reagent grade NaCl and doubly-deionized water ( $\mu < 1\mu\text{mhos}$ ). Commercial grade CO<sub>2</sub> (CO<sub>2</sub> > 99%) was used to maintain a CO<sub>2</sub> atmosphere over the solutions during experimentation.

An Orion 901 pH meter and research grade pH electrode (Orion 91-02) were used to measure the pH. The electrode was periodically calibrated to within  $\pm 0.02$  pH units using Fisher gram-pac buffers (pH 4.01 and 6.86 at 25°C).

Magnesium concentrations were measured by EDTA complexometric titration (Skoog and West, 1974). EDTA solutions were prepared from oven-dried reagent grade solid, and standardized against Fisher Mg standard solution (Mg = 1000  $\pm$  10 ppm). Eriochrome Black T was used as an endpoint indicator.

All glassware and pipets were class A and calibrated prior to use. Eppendorf digital pipets were accurate to  $\pm 1$  percent. A Sartorius analytical balance was used for all weighings. Calibration of the balance against standard weights showed it accurate to  $\pm 0.0003$  grams between 0.0001-160.0000 grams. Thermometers were found to be accurate to  $\pm 0.1^{\circ}\text{C}$  over a temperature interval of 0 to  $100^{\circ}\text{C}$ .

Solubility experiments were performed in 1 liter pyrex reaction cells, prewashed with 1:1  $\text{HNO}_3$  then rinsed several times with deionized water. Silicone grease was applied to the ground-glass lips of the cells and the cells then sealed with plexiglas covers. Four holes in each cover allowed for the insertion of a coarse-fritted glass gas dispersion tube and the periodic insertion of a pH electrode. Gum rubber stoppers sealed the remaining holes.

Solutions ranging in ionic strength from 0 to 5.5 molal were prepared by dissolving oven-dried reagent grade NaCl in volumetrically measured quantities of doubly-deionized water. Density corrections were made to compute the concentrations in molal units. The solutions were added to each reaction cell along with approximately 20 grams of nesquehonite.

A  $\text{CO}_2$  atmosphere was maintained in the cells throughout

the solubility runs, which were maintained at a total pressure equal to the ambient barometric pressure of about 0.8 atm. Carbon dioxide gas presaturated with water vapor was passed through the gas dispersion tube and allowed to exit through a small hole in one of the gum stoppers.

Barometric pressure, measured periodically and at the end of the experiments, varied a maximum of  $\pm 3.5$  mm (615 to 622 mm Hg total pressure), which when corrected for  $P(\text{H}_2\text{O}) = 0.031$  atm, gave  $P(\text{CO}_2) = 0.78 \pm 0.01$  atm.

Throughout the experiments the solutions were stirred with a suspended teflon-coated magnetic stirbar specifically designed to avoid grinding of the solid. The reaction cells were placed in a water bath and one set of solubility runs maintained at  $25.0 \pm 0.1^\circ\text{C}$ . The pHs were measured periodically during the experiments. When pH no longer changed between several measurements it was judged that equilibrium had been attained. Equilibrium in the  $25^\circ\text{C}$  solubility experiments was approached from undersaturation. Since nesquehonite has the typical carbonate inverse solubility with temperature, reversal of the  $25^\circ\text{C}$  experiments was attempted by lowering the temperature to  $15^\circ\text{C}$  for 1-3 days, then returning the samples to  $25^\circ\text{C}$  and monitoring the pH.

Nesquehonite solubility runs in NaCl solutions were

also performed at 15 and 35°C. In the 15°C solubility run, equilibrium was reached from undersaturation. Equilibrium in the 35°C run was approached initially from 25°C, and therefore from supersaturation. No attempt was made to reverse the 15°C experiment.

Most solubility runs were completed in 1 to 3 weeks. After termination of the experiments, aliquots were withdrawn and filtered through 0.2µm polycarbonate millipore filters using a polycarbonate filter holder to assure complete removal of fine particulates. These aliquots were analyzed for Mg by EDTA titration.

### Results

The final molal magnesium concentration, ionic strength and measured equilibrium pH for the nesquehonite solubility experiments in NaCl solutions are given in Tables 5-7. The results show the expected decrease in magnesium concentration with increasing temperature. Measured pHs in the solubility experiments were corrected for liquid junction potentials with the Henderson equation, assuming a saturated KCl salt bridge (Bates, 1973).

The solubility of nesquehonite can be written

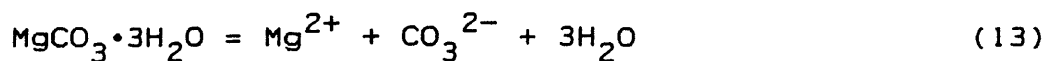


Table 5. Final Mg concentrations, ionic strengths and equilibrium pH for nesquehonite solubility experiments run from undersaturation, at 15°C and  $P(\text{CO}_2) = 0.78$  atm. Analytical precision is approximately  $\pm 5$  percent.

m NaCl	I (m)	m $\text{Mg}^{2+}$	pH
0.0	0.515	0.176	7.22
0.1	0.560	0.169	7.08
0.3	0.783	0.171	7.08
0.5	1.01	0.178	7.07
0.75	1.25	0.170	7.02
1.0	1.49	0.164	6.98
1.5	2.02	0.169	6.96
3.5	4.01	0.138	6.81
4.5	5.03	0.120	6.77

Table 6. Final Mg concentrations, ionic strength and equilibrium pH for reversed nesquehonite solubility experiments at 25°C and  $P(\text{CO}_2) = 0.78$  atm. Uncertainties were obtained from replicate experiments. Analytical precision is approximately  $\pm 5$  percent.

m NaCl	I (m)	m $\text{Mg}^{2+}$	pH
0.0	0.483	0.161 $\pm$ 0.008	7.16
0.1	0.619	0.173 $\pm$ 0.002	7.15
0.3	0.819	0.173 $\pm$ 0.008	7.14
0.5	1.06	0.186 $\pm$ 0.003	7.13
0.75	1.28	0.176 $\pm$ 0.050	7.10
1.0	1.59	0.195 $\pm$ 0.001	7.10
1.5	2.04	0.181 $\pm$ 0.010	7.07
2.0	2.58	0.185 $\pm$ 0.003	7.06
2.5	3.06	0.186 $\pm$ 0.002	7.01
3.0	3.54	0.170 $\pm$ 0.010	6.96
3.5	3.94	0.147 $\pm$ 0.007	6.97
4.0	4.46	0.139 $\pm$ 0.010	6.97
4.5	4.91	0.136 $\pm$ 0.005	6.87
5.0	5.48	0.144 $\pm$ 0.010	6.88
5.5	5.88	0.127 $\pm$ 0.001	6.85

Table 7. Final Mg concentrations, ionic strength, and equilibrium pH of the nesquehonite solubility experiments run from supersaturation at 35°C and  $P(\text{CO}_2) = 0.78$  atm. Analytical precision is approximately  $\pm 5$  percent.

m NaCl	I (m)	m $\text{Mg}^{2+}$	pH
0.0	0.457	0.159	7.27
0.1	0.528	0.151	7.20
0.3	0.739	0.152	7.17
0.5	0.984	0.164	7.18
0.75	1.23	0.161	7.14
1.0	1.47	0.152	7.10
1.5	2.02	0.160	7.10
3.5	3.99	0.120	6.92
4.5	4.99	0.107	6.84

Using an ion association approach to the computation, the solubility product of nesquehonite at 25°C was computed from the magnesium concentration in the NaCl-free solubility run reported in Table 6, by an iterative technique. The formation of ion pairs reduces the concentrations of free magnesium and carbonate species as well as the ionic strength. Values of  $\gamma(\text{Mg}^{2+})$ , and  $\gamma(\text{HCO}_3^-)$  used in the computation were obtained from mean salt calculations using data from Goldberg and Nuttall (1978) and Roy et al. (1983). Computational methods are described by Garrels and Christ (1965). The values for  $\gamma(\text{MgCO}_3^0)$ ,  $\log K(\text{MgHCO}_3^+) = -0.97$  and  $\log K(\text{MgCO}_3^0) = -2.33$  were obtained from Reardon (1974) and Reardon and Langmuir (1974). Bicarbonate and carbonate ion activities were computed from the pH and  $P(\text{CO}_2)$ .

The results of these calculations lead to an effective  $I = 0.36$  and  $\log K_{sp} = -5.44$  at 25°C. This value is in good agreement with the solubility work of Hostetler as reported by Robie and Hemingway (1983) who found  $\log K_{sp} = -5.42$ . A similar calculation of  $K_{sp}$  was made based on the 25°C solubility reported by Langmuir (1965) for  $P(\text{CO}_2) = 0.97$  atm, for which he reported a solution pH of 7.11 and  $m \text{Mg}^{2+} = 0.213$ . This leads to  $\log K_{sp} = -5.53$ . The NBS value of  $\log K_{sp} = -5.60$ , reported by Wagman et al. (1982) is most likely a recomputation of the Langmuir (1965) work.

These results are in poor agreement with Ming (1980), who obtained  $\log K_{sp} = -5.80 \pm 0.10$ . However, Ming worked at low  $\text{CO}_2$  pressures ( $\log P(\text{CO}_2) = -3.6$  atm); conditions which plot in the hydromagnesite field (Figure 1). Ming measured  $\text{Mg}^{2+}$  and pH in a system in which he had precipitated nesquehonite from a saturated hydromagnesite solution at one atmosphere  $\text{CO}_2$  and allowed the system to degas for one year at  $25^\circ\text{C}$ . He identified nesquehonite as the solid phase present both after initial precipitation and after the one year period. However, its presence does not prove the solution was in equilibrium with this phase. The transformation of solid nesquehonite to hydromagnesite may be kinetically unfavorable.

Hostetler (as reported by Robie and Hemingway, 1973) obtained  $\log K_{sp} = -5.42 \pm 0.1$  from pH measurements of a nesquehonite saturated solution under a saturated  $\text{CO}_2$  atmosphere. Robie and Hemingway (1973) themselves reported  $\log K_{sp} = -5.06 \pm 0.18$  computed from calorimetric measurements. The  $\log K_{sp}$  values at 15 and  $35^\circ\text{C}$  were computed by correcting the literature values using the van't Hoff equation assuming  $\Delta C_p^\circ = 0$  for the dissolution of nesquehonite and  $\Delta H_f^\circ = -472.576$  kcal/mol for the nesquehonite solid phase (Robie and Hemingway, 1973).

The values of  $\log K_{sp}$  at 15, 25 and  $35^\circ\text{C}$  are given in

Table 8. Inspection of the 25°C  $K_{sp}$ 's reveals three closely spaced values, all of which were determined by direct solubility methods. The two other values were obtained by indirect methods. It is not clear how  $K_{sp}$  was calculated from the solubility measurements of Hostetler so this result is suspect. Therefore the recommended value for the  $K_{sp}$  of nesquehonite at 25°C has been calculated as the average of -5.53 and -5.44 which is  $-5.48 \pm 0.06$ .

Currently the Pitzer ion-interaction model contains parameters for the magnesium carbonate system from Harvie et al. (1984). The activities of water and magnesium computed using these parameters and assuming  $m\text{HCO}_3^- = 2m\text{Mg}^{2+}$  from the charge balance are given in Tables 9-11.

Mean activity coefficients of  $\text{MgCl}_2$  computed for the 25°C solubility experiments were compared with their values for pure  $\text{MgCl}_2$  solutions as reported by Goldberg and Nuttall (1978). Values from the two approaches were within 0.02 units of each other up to  $I = 4.0m$ . Differences between the mean activity coefficients increased at higher ionic strength. This would indicate that the major effect of ionic strength on the activity of  $\text{Mg}^{2+}$ , even in the presence of equal concentrations of  $\text{HCO}_3^-$ , is accounted for in the Mg-Cl parameters.

By combining the carbonate equilibrium expressions with

Table 8. Values of Log Ksp for nesquehonite at 15, 25 and 35°C computed using  $\Delta H_f^\circ = -472.576$  kcal/mol from Robie and Hemingway (1973) and assuming  $\Delta C_p^\circ = 0$  for the dissolution of nesquehonite.

15°C	25°C	35°C	Reference
-5.38	-5.53	-5.67	Langmuir (1965)
-4.91	-5.06	-5.20	Robie and Hemingway (1973)
-5.27	-5.42	-5.56	Hostetler(1973)
-5.65	-5.80	-5.94	Ming(1982)
-5.29	-5.44	-5.58	This study (computed)

Table 9. Pitzer model computed activities of  $Mg^{2+}$ ,  $CO_3^{2-}$  and  $H_2O$  and log IAP of nesquehonite for the  $15^\circ C$  solubility run approached from undersaturation.

m NaCl	$[Mg^{2+}]$	$[CO_3^{2-}](\times 10^4)$	$[H_2O]$	log IAP
0.0	0.0271	1.39	0.993	-5.43
0.1	0.0262	0.732	0.991	-5.73
0.3	0.0273	0.776	0.984	-5.69
0.5	0.0294	0.770	0.977	-5.68
0.75	0.0308	0.636	0.969	-5.75
1.0	0.0327	0.543	0.960	-5.80
1.5	0.0414	0.519	0.942	-5.75
3.5	0.0973	0.289	0.867	-5.74
4.5	0.1560	0.246	0.827	-5.66
			mean log IAP value	$-5.69 \pm 0.11$

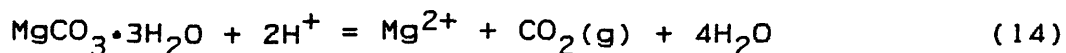
Table 10. Pitzer model computed activities of  $Mg^{2+}$ ,  $CO_3^{2-}$  and  $H_2O$  and log IAP of nesquehonite for the  $25^\circ C$  reversed solubility run.

m NaCl	$[Mg^{2+}]$	$[CO_3^{2-}](\times 10^4)$	$[H_2O]$	log IAP
0.0	0.0249	1.13	0.993	-5.54
0.1	0.0256	1.06	0.989	-5.57
0.3	0.0262	1.02	0.983	-5.57
0.5	0.0286	0.959	0.976	-5.57
0.75	0.0298	0.832	0.968	-5.62
1.0	0.0347	0.812	0.959	-5.58
1.5	0.0407	0.715	0.942	-5.60
2.0	0.0540	0.675	0.923	-5.55
2.5	0.0663	0.522	0.905	-5.58
3.0	0.0830	0.422	0.885	-5.64
3.5	0.0940	0.436	0.866	-5.59
4.0	0.130	0.420	0.845	-5.53
4.5	0.148	0.253	0.842	-5.64
5.0	0.234	0.264	0.800	-5.56
5.5	0.255	0.223	0.778	-5.56
mean log IAP value				$-5.58 \pm 0.03$

Table 11. Pitzer model computed activities of  $\text{Mg}^{2+}$ ,  $\text{CO}_3^{2-}$  and  $\text{H}_2\text{O}$  and the log IAP of nesquehonite for the  $35^\circ\text{C}$  solubility run approached from supersaturation.

m NaCl	$[\text{Mg}^{2+}]$	$[\text{CO}_3^{2-}](\times 10^4)$	$[\text{H}_2\text{O}]$	log IAP
0.0	0.0239	1.95	0.994	-5.34
0.1	0.0231	1.45	0.991	-5.49
0.3	0.0234	1.33	0.984	-5.53
0.5	0.0255	1.44	0.977	-5.47
0.75	0.0269	1.25	0.969	-5.51
1.0	0.0280	1.07	0.960	-5.58
1.5	0.0355	1.13	0.942	-5.47
3.5	0.0709	0.545	0.867	-5.60
4.5	0.108	0.378	0.826	-5.64
		mean log IAP value $-5.51 \pm 0.09$		

The solubility expression for nesquehonite, the proton form of the nesquehonite solubility equation becomes



and the equilibrium constant expression can be written

$$K_{sp} = [\text{Mg}^{2+}] P(\text{CO}_2) [\text{H}_2\text{O}]^4 / [\text{H}^+]^2 K_h K_1 K_2 \quad (15)$$

Using the Pitzer model derived activities for the solubility experiments, the ion activity products (IAP's) were computed. Under equilibrium conditions, which is assumed for these experiments, the IAP is equal to the  $K_{sp}$ . The results are given in Tables 9-11.

The Pitzer ion approach uses the total ionic strength, and does not adjust the free magnesium and carbonate or ionic strength by assuming ion pairs. The result is that although the  $K_{sp}$ 's obtained from the different approaches are comparable, the activity coefficients are quite different. The Pitzer approach to nesquehonite solubility in  $\text{CO}_2$ -saturated water at  $25^\circ\text{C}$  gives a stoichiometric  $I = 0.483$  and  $\log K_{sp} = -5.54$ , which is in good agreement with the recomputed Langmuir (1965)  $K_{sp}$  value. Although magnesium concentrations show their expected decrease with

increasing temperature, the  $K_{sp}$  values obtained from the Pitzer equations increase with increasing temperature. This result is impossible to explain given a negative enthalpy of reaction for equation 13. When using only the 25°C data the result is  $\log K_{sp} = -5.58 \pm 0.03$ . This average is in reasonable agreement with the new Langmuir (1965) value but is quite lower than the value obtained from the deionized water experiment.

### Conclusions

As expected, the ion association and ion interaction approaches give comparable results for the low ionic strength waters. The results of the nesquehonite solubility experiments, although not accurate enough to compute refined Mg-HCO<sub>3</sub> parameters, indicate that the Pitzer ion interaction model is capable of computing approximate  $\gamma$ 's for the Mg-HCO<sub>3</sub>-CO<sub>3</sub>-H<sub>2</sub>O system up to  $I = 5.5$ . Given the uncertainties associated with field sampling of these types of waters, the model should be sufficiently accurate for application to the brines of the Palo Duro basin.

## PALO DURO BASIN BRINES STUDY

Geology and Hydrology

The study area for this research is the Palo Duro basin of north Texas (Figure 2). The basin is approximately 200 km from north to south and 250 km from east to west. Total sediment thickness ranges from about 3000 m near the center of the basin, to about 500-700 m above the northern basin margin, and 2000 m over the southern basin margin. Detailed geologic cross-sections have been published by Bassett and Bentley (1982, 1983). The geology and hydrology has been more fully described by Langmuir and Melchior (1985).

The majority of brine samples were collected from two horizons, the granite wash and carbonates of the Wolfcamp Formation. Samples were also collected from the Pennsylvanian carbonate, the Ellenberger carbonate and the Ellenberger sand. These formations lie approximately 800 m below the San Andres salt beds which were considered a potential host rock for a high-level nuclear waste repository. They are the most permeable and porous aquifers below the San Andres formation and therefore could facilitate the migration of radionuclides if a repository breach occurred.

The granite wash facies is a detrital sediment of late

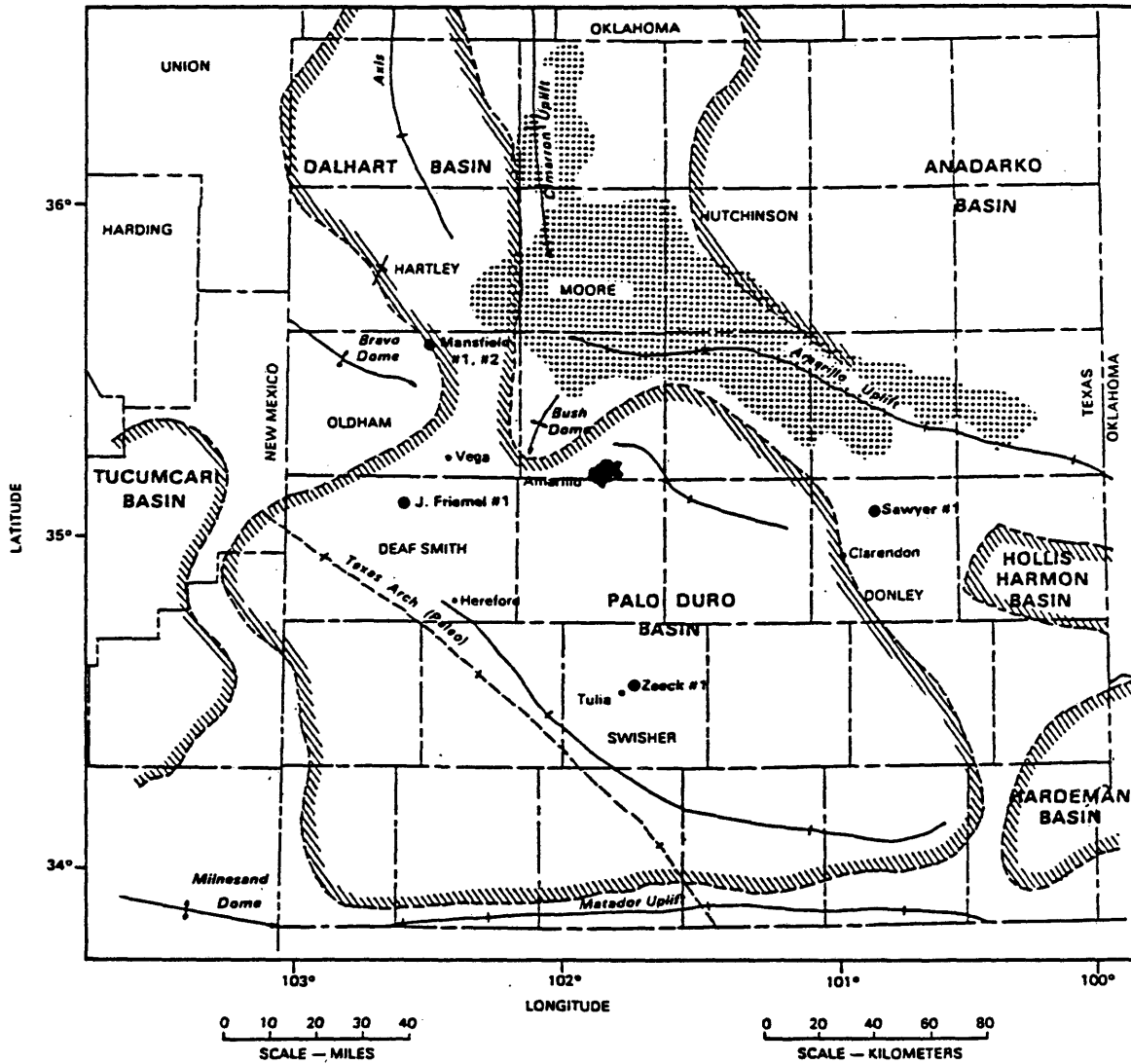


Figure 2. The Palo Duro basin and the locations of the sample wells. (taken from Zaikowski et al., 1987)

Pennsylvanian and early Permian age. The granite wash ranges from arkosic sandstone to conglomerate. The sediments were cemented early in their history by calcite, ankerite, ferroan calcite, quartz, K-feldspar and kaolinite (Dutton, 1982). The granite wash ranges in thickness from 70 to 130 m over the areas sampled.

The Wolfcamp Formation was formed as reef and shelf carbonates during the early Permian. It is composed of calcites and dolomites interbedded with black shales near the basin center. The Wolfcamp is considerably thicker than the granite wash and in the study area ranges from 300 to over 600 m thick. Petrographic and mineralogical analysis of Wolfcamp cores has been published by Fukui and Dayvault (1985). An abbreviated description of the petrology of the cores from Smith et al. (1985) is given in Table 12.

Potentiometric maps for the Wolfcamp Formation are given by Bassett and Bentley (1982). The maps indicate a generally east to north-east ground water flow entering from the western basin margin. Water level information for the granite wash, though sparse, indicates lower heads with gradients and direction of flow similar to the Wolfcamp. No data is available for the Pennsylvanian carbonates.

Total potentiometric heads in the Wolfcamp and granite wash are greater than the elevation heads, indicating

Table 12. A brief description of the major lithologic components of the Palo Duro cores, based on Smith et al. (1985).

#### Mansfield Well

- Zone 2: Principally organic-rich fossiliferous limestones with some dolomite.
- Zone 1: Fossiliferous limestone with some organics and yellow staining.

#### Zeeck Well

- Zone 3: Organic rich fossiliferous limestone and dolomite. Some fracture filling by anhydrite. Some pyrite present.
- Zone 2: Fossiliferous dolomite with some limestone. Fossils filled with anhydrite and pyrite. Interval is bounded by thick claystone beds.

#### J. Friemel Well

- Zone 7: Fossiliferous limestone with minor dolomite. Fossils contain anhydrite and silica.
- Zone 6: No data available.
- Zone 5: Arkosic sand and gravel with carbonate cements.
- Zone 4: No data available.
- Zone 3: Arkosic coarse sandstone and gravel with calcite cement.
- Zone 2 : Coarse to fine sandstone with some anhydrite cements. Some pyrite, organic stains and mud.
- Zone 1: Sands and gravels with dolomite cement. Pyrite and some mudstone present.

(continued)

Table 12. (continued)

Sawyer Well

Zone 1-4: No petrologic data available.

Zone 5 : Principally dolomite with some limestone showing fine sand sized allochems.

artesian conditions. The water levels in the wells screened in these formations rise above the level of the Permian salt beds. This indicates a general upward movement of basin groundwaters towards the Permian evaporites. Finite element modelling of groundwater flow results in an average age of 170 million years for the Wolfcamp and 188 million years for the granite wash (Atwood and Pickering, 1986). Radiometric age dating using  $^4\text{He}$  from the decay of U and Th, and  $^{40}\text{Ar}$  from  $^{40}\text{K}$  decay give a preferred age of 100 million years for the Wolfcamp brines (Zaikowski et al., 1984).

#### Chemistry of the Palo Duro Brines

Seventeen samples were collected by Bendix Field Engineering in 1981 and 1982 from four DOE wells in the Palo Duro basin (Figure 2). The geologic units sampled, their lithology, the depth interval sampled, temperature, and shut-in pressures are given in Tables 13 and 14 (cf. Smith et al., 1985). A thiocyanate tracer was added to the drilling fluid and its concentration monitored during the pumping of the well. Water samples were collected only after the tracer concentration had decreased to less than 0.5 % of its initial value (Hubbard, 1984). Samples were field-filtered through a 0.45 um filter and acidified with nitric acid. Five of the samples from the Mansfield, Sawyer

Table 13. DOE wells in the Palo Duro basin, Texas, and their units, major lithologies, and depths sampled.

<u>Well</u>	<u>Zone</u>	<u>Unit</u>	<u>Lithology</u>	<u>Depth (ft)</u>
Sawyer	1	Ellenberger	Sand	4716-4746
	2	Ellenberger	Carbonate	4604-4640
	3	Mississippian	Carbonate	4500-4535
	4	Pennsylvanian	Granite wash	4258-4342
	5	Wolfcamp	Carbonate	3172-3189
Mansfield	1	Wolfcamp	Carbonate	4818-4890
	2	Wolfcamp	Carbonate	4514-4638
Zeeck	1	Pennsylvanian	Carbonate	7140-7152
				7172-7230
	2	Wolfcamp	Carbonate	5603-5625
				5630-5640
	3	Wolfcamp	Carbonate	5542-5550
				5500-5538
			5470-5496	
J. Friemel	1	Pennsylvanian	Granite Wash	8168-8204
	2	Pennsylvanian	Granite Wash	8122-8132
	3	Pennsylvanian	Granite Wash	8040-8050
	4	Pennsylvanian	Granite Wash	7896-7904
	5	Pennsylvanian	Granite Wash	7729-7734
	6	Pennsylvanian	Carbonate	7360-7362
	7	Wolfcamp	Carbonate	5825-5926

Table 14. Temperatures and pressures in the Palo Duro sampling intervals.

<u>Well</u>	<u>Zone</u>	<u>Temperature (<math>^{\circ}</math>C)</u>	<u>Pressure (bars)</u>
Sawyer	1	39	-
	2	39	-
	3	39	79
	4	39	74
	5	35	62
Mansfield	1	38	84
	2	41	77
Zeeck	1	56	173
	2	38	117
	3	41	130
J Friemel	1	55	193
	2	55	191
	3	55	189
	4	55	185
	5	53	179
	6	52	165
	7	38	116

and Zeeck wells were analysed by Bendix Field Engineering. All seventeen samples were analysed by the Texas Bureau of Economic Geology (TBEG) and the results reported by Fisher and Krietler (1985). Measured concentrations are considered accurate to 10% or better.  $^{226}\text{Ra}$  was analysed by Laul and others (1984). Molal concentrations determined using measured densities are given in Table 15. Some analytical differences between the TBEG and Bendix results were found in the five duplicated analyses.

Of particular interest for this study is the carbonate system. Unfortunately there are several problems with the field collected data. The alkalinities are very likely too high due to the presence of titratable short chain organic acids which were later semi-quantified (J. Means, personal communication). In addition, significant degassing of  $\text{CO}_2$  from the samples probably occurred prior to the alkalinity determinations. The pH data is also suspect due to this  $\text{CO}_2$  degassing. Oxidation of  $\text{Fe}^{2+}$  and precipitation of ferric hydroxide may have occurred in some samples which resulted in a drop in the solution pH.

Concentrations of  $\text{Na}^+$  and  $\text{Cl}^-$  lack any significant trends with depth.  $\text{Ca}^{2+}$  and  $\text{Sr}^{2+}$  concentrations increase with depth.  $\text{Ca}^{2+}$  is approximately two orders of magnitude greater than  $\text{Sr}^{2+}$ , but the relative magnitude of their

Table 15. Molal concentrations of major chemical species in the Palo Duro brines computed from data of Fisher and Krietler (1985). Analytical precision is approximately  $\pm 10$  percent.

Well/Zone	Na	K (x100)	Ca (x100)	Mg	Sr (x100)	Cl	SO <sub>4</sub> (x100)	HCO <sub>3</sub>	pH
<b>Sawyer</b>									
1	2.88	1.28	0.627	0.117	0.827	4.30	0.193	1.01	5.3
2	3.04	1.17	0.590	0.127	0.886	4.10	0.252	0.072	7.5
3	2.90	0.942	0.529	0.104	0.716	4.07	0.270	0.190	5.4
4	3.02	0.929	0.500	0.098	0.704	4.20	0.383	0.047	4.4
5	2.00	0.320	0.179	0.108	0.137	2.58	2.21	0.250	6.1
<b>Mansfield</b>									
1	3.73	1.03	0.163	0.059	0.125	4.26	1.39	0.236	5.6
2	3.61	1.06	0.164	0.072	0.112	4.03	1.49	0.288	4.8
<b>Zeeck</b>									
1	3.71	0.563	0.333	0.712	1.76	4.77	0.094	0.057	5.8
2	2.88	0.861	0.181	0.057	0.306	3.18	1.09	0.198	6.9
3	3.26	0.938	0.169	0.081	0.136	3.66	1.86	0.168	6.2

(continued)

Table 15. (continued).

Well/Zone	Na	K (x100)	Ca (x100)	Mg	Sr (x100)	Cl	SO <sub>4</sub> (x100)	HCO <sub>3</sub>	pH
J. Friemel									
1	3.77	1.77	0.436	0.097	0.564	4.66	0.510	0.064	5.9
2	3.78	1.73	0.427	0.097	0.532	4.64	0.563	0.126	5.9
3	3.74	1.81	0.417	0.100	0.520	4.62	0.569	0.129	6.0
4	3.78	1.66	0.478	0.117	0.576	4.95	0.604	0.038	6.2
5	4.33	2.73	0.549	0.141	0.742	5.73	0.448	0.080	5.2
6	3.80	2.57	0.355	0.117	0.461	4.74	0.732	0.134	6.4
7	3.43	1.64	0.228	0.097	0.186	3.99	1.56	0.366	4.2

concentration increases with depth are similar. The Zeck well, zone 1 has an anomalously high  $\text{Sr}^{2+}$  concentration in comparison to the other samples.  $\text{Mg}^{2+}$  lacks a trend with depth except for one anomalously high value in Zeck well, zone 1. Sulfate decreases with depth with a very low concentration in the Zeck well, zone 1. Alkalinity (expressed as  $\text{HCO}_3^-$ ) and pH show considerable variation and no trends with depth. This behavior is probably an artifact of the sampling and analytical problems described above.

#### Temperature and pressure effects

The brines of the Palo Duro basin are at elevated temperatures and pressures (Table 14). The effect of pressure and temperature on the activity coefficients must be known in order to use the Pitzer model for this system. To compute the sulfate and carbonate mineral saturation states, the solubilities of these minerals must also be corrected to in-situ temperatures and pressures of the Palo Duro basin.

It has been found that when considering the effects of temperature and pressure on the ion-interaction parameters, only temperature effects are significant (cf. Pitzer, 1979). Rogers (1981) has shown that the Debye-Huckel  $A_\phi$  parameter, increases by only three percent between 1 and 600 bars. The

highest pressure measured in the Palo Duro samples was 193 bars. For this reason the effect of pressure on the activity coefficients predicted by the Pitzer model was judged insignificant.

The effect of temperature on  $A_{\text{O}}$  (Pitzer, 1979) is:

$$A_{\text{O}} = 0.3769 + 4.724 \times 10^{-4}T + 3.8 \times 10^{-6}T^2 \quad (16)$$

Temperature derivatives of the ion interaction parameters are known for only a few components in the Pitzer data base. Melchior (1984) compared the effect of temperature on the  $A_{\text{O}}$  parameter to the temperature derivatives of the ion-interaction parameters. He found that the increase in the  $A_{\text{O}}$  parameter with increasing temperature was responsible for 98 percent of the change in the activity coefficient of  $\text{Ca}^{2+}$  at  $100^{\circ}\text{C}$ . From this result it was inferred by the author that the Pitzer model would accurately predict activity coefficients at temperatures up to  $100^{\circ}\text{C}$  for all the components in the data base, including those for which the temperature derivatives of the ion-interaction parameters are not known.

The effect of temperature on the solubilities of calcite, aragonite, and vaterite ( $\text{CaCO}_3$ ); strontianite ( $\text{SrCO}_3$ ); and witherite ( $\text{BaCO}_3$ ) were published by Plummer and

Busenburg (1982), Busenberg et al. (1984) and Busenberg and Plummer (1986). For calcite between 0 and 90°C the expression is:

$$\log K_{sp} = -171.9065 - 0.077993T + 2839.319/T + 71.595 \log T \quad (17)$$

for strontianite between 2 and 91°C:

$$\log K_{sp} = 155.0305 - 72399.594/T - 56.58638 \log T \quad (18)$$

and for witherite between 0 and 90°C:

$$\log K_{sp} = 607.642 + 0.121098T - 20011.25/T - 236.4948 \log T \quad (19)$$

Langmuir and Melchior (1985) recomputed temperature and pressure functions for the solubility products of gypsum, anhydrite, celestite, and barite. For gypsum between 25 and 90°C the expression is:

$$\log K_{sp} = 68.2401 - 3221.51/T - 25.0627 \log T \quad (20)$$

for anhydrite the expression fit from 70 to 150°C and

extrapolated to 25°C is:

$$\log K_{sp} = 87.805 - 3210.8/T - 32.8461 \log T \quad (21)$$

for celestite between 20 and 100°C:

$$\log K_{sp} = 137.555 - 6530.75/T - 49.419 \log T \quad (22)$$

and for barite from Blount (1977) from 22 to 280°C and pressures from 1 to 1400 bars:

$$\log K_{sp} = (1.49325 \times 10^{-2} P - 48.61) \log T + (2.35365 P - 7682.76)/T - 4.398 \times 10^{-2} P + 136.079 \quad (23)$$

The temperature function for dolomite solubility was published by Langmuir (1984) and is:

$$\log K_{sp} = 23.694 - 0.07965T - 5052.9/T \quad (24)$$

The effect of pressure on mineral solubility has been examined by several authors (Lown et al, 1968; Macdonald and North, 1974; Millero, 1982). In general the effect of pressure is given by

$$\ln(K^P/K^0) = - dV P/RT + 0.5 dK P^2/RT \quad (25)$$

where P = pressure, T = absolute temperature, dV = the change in total molar volume, and dK = the change in total molar compressibility (Millero, 1982). These total molar values are the sum of the partial molar values (Millero, 1982). Equation 25 was used to calculate the effect of pressure on the solubility products of calcite, dolomite, strontianite, and anhydrite.

The equations of Blount and Dickson (1973) were used for gypsum and anhydrite. For anhydrite the expression is

$$\begin{aligned} \ln m = & -2.87 + 1.220 \times 10^{-3}P - 0.0237T - 0.0028 \times 10^{-3}PT \\ & + 0.010 \times 10^{-4}T^2 + 0.140 \times 10^{-7}PT^2 \end{aligned} \quad (26)$$

and for gypsum

$$\begin{aligned} \ln m = & -4.355 + 0.840 \times 10^{-3}P + 0.0105T - 1.700 \times 10^{-4}T^2 \\ & + 0.584 \times 10^{-6}T^3 \end{aligned} \quad (27)$$

where m = the molar solubility. After the molar solubility of anhydrite and gypsum are computed for elevated pressures, their solubility products are calculated using the Pitzer model.

For celestite the equation of MacDonald and North (1974) was used:

$$d \log K / dP = 8.576 \times 10^{-4} P \quad (28)$$

#### Mineral saturation in the Palo Duro brines

After determining the effects of temperature and pressure on mineral solubilities as described above, the molal concentrations given in Table 15 were converted to activities using the Pitzer model, these are given in Table 16. The results were used with the measured pH and alkalinity or  $P(\text{CO}_2)$  data and corrected mineral solubilities to compute IAPs for the minerals. The saturation index (SI) then computed equals  $-\log (IAP/K_{sp})$ . Results of these calculations are given in Table 17.

Using the measured pH and  $P(\text{CO}_2)$  data the carbonate minerals range from undersaturation to supersaturation in the brines. Due to the problems noted in the carbonate analytical data, the assumption of calcite saturation was then made. This is believed a viable assumption for two reasons. One is that all the core materials in contact with the water samples contained some calcite and/or dolomite. Secondly, because of the slow flow rates (0.9 to 9 cm/yr; Langmuir and Melchior, 1985) there has been ample time for

Table 16. Molal activities of the major species in the Palo Duro brines computed using the Pitzer equations.

Well	Na	K ( $\times 10^3$ )	Ca ( $\times 10$ )	Mg ( $\times 10^2$ )	Sr ( $\times 10^3$ )	Cl	SO <sub>4</sub> ( $\times 10^5$ )
J. Friemel							
1	3.03	8.13	1.61	5.12	1.88	5.04	12.6
2	3.01	44.5	1.52	4.95	1.81	5.04	14.2
3	3.00	8.36	1.54	5.13	1.73	4.92	14.2
4	3.15	7.63	2.02	7.27	2.18	5.48	13.9
5	3.93	12.3	3.24	13.1	3.78	7.06	9.17
6	3.12	12.1	1.50	7.17	1.71	4.92	17.8
7	2.58	7.75	0.867	5.19	0.579	3.65	42.4
Zeeck							
1	2.73	2.13	0.908	2.79	4.32	7.44	3.05
2	2.00	4.15	0.506	2.10	0.728	2.65	35.8
3	2.41	4.55	0.568	3.74	0.386	3.17	54.8
Sawyer							
1	2.12	5.50	2.23	6.05	2.42	4.70	4.83
2	2.16	4.95	1.80	5.58	2.24	4.60	6.87
3	2.10	4.15	1.76	4.95	1.98	4.21	7.09
4	2.24	4.15	1.82	5.17	2.11	4.29	9.72
5	1.31	1.55	0.426	3.27	0.283	2.03	81.5

(continued)

Table 16. (continued).

Well	Na	K ( $\times 10^3$ )	Ca ( $\times 10$ )	Mg ( $\times 10^2$ )	Sr ( $\times 10^3$ )	Cl	SO <sub>4</sub> ( $\times 10^5$ )
Mansfield							
1	2.79	5.17	0.653	4.02	0.371	3.57	40.7
2	2.97	5.08	0.768	4.04	0.475	3.74	35.2

Table 17. Saturation indices for selected minerals in the Palo Duro brines computed using Pitzer equations.

Well	CaCO <sub>3</sub>	CaMg(CO <sub>3</sub> ) <sub>2</sub>	CaSO <sub>4</sub>	CaSO <sub>4</sub> •2H <sub>2</sub> O	SrSO <sub>4</sub>	BaSO <sub>4</sub>	RaSO <sub>4</sub>
Sawyer							
1	+0.51	+0.68	-0.53	-0.56	-0.36	-	-
2	+1.47	+2.65	-0.57	-0.50	-0.24	-	-
3	-0.24	-0.79	-0.55	-0.49	-0.28	-	-
4	-1.85	-4.03	-0.40	-0.34	-0.11	+0.34	-6.33
Mansfield							
1	-0.53	-1.13	-0.24	-0.17	-0.21	-0.65	-6.22
2	-1.24	-2.45	-0.20	-0.16	-0.25	-0.20	-6.16
Zeeck							
1	-0.63	-0.32	-0.02	-0.20	-0.33	-	-
2	+0.61	+1.06	-0.43	-0.31	-0.04	-	-
3	-0.09	-0.11	-0.17	-0.10	-0.14	-1.44	-5.77

(continued)

Table 17. (continued).

Well	CaCO <sub>3</sub>	CaMg(CO <sub>3</sub> ) <sub>2</sub>	CaSO <sub>4</sub>	CaSO <sub>4</sub> •2H <sub>2</sub> O	SrSO <sub>4</sub>	BaSO <sub>4</sub>	RaSO <sub>4</sub>
J. Friemel							
1	-0.26	-0.64	-0.14	-0.28	-0.11	-	-
2	-0.04	-0.13	-0.12	-0.25	-0.06	-	-
3	+0.10	+0.14	-0.11	-0.24	-0.08	-	-
4	-0.11	-0.24	0.00	-0.15	+0.01	-	-
5	-0.67	-1.33	-0.04	-0.20	+0.07	-	-
6	+0.45	+0.97	-0.09	-0.20	+0.02	-	-
7	-1.65	-3.32	-0.13	-0.04	-0.07	-	-

equilibrium with calcite to be reached. With the assumption of calcite saturation and the activity of  $\text{Ca}^{2+}$  known, it is possible to fix the activity of  $\text{CO}_3^{2-}$  and thereby compute the saturation state of the other carbonate minerals. These results are given in Table 18.

Dolomite is now near saturation in all samples with the exception of the Sawyer well which shows a slight increase in undersaturation with depth. That dolomite is computed to be at saturation adds validity to the assumption of calcite saturation. Strontianite is now undersaturated in all of the wells by approximately 1.1 to 1.5 orders of magnitude. It is somewhat closer to saturation in the Zeck well, zone 1, which is likely the result of the anomalously high  $\text{Sr}^{2+}$  concentration in this zone. This relatively constant degree of undersaturation could indicate a solid solution of  $\text{Sr}^{2+}$  in calcite. However, there is no direct evidence for this in these samples. Very little analytical data exists for  $\text{Ba}^{2+}$  or  $\text{Ra}^{2+}$  in this system.

Gypsum and anhydrite show increasing undersaturation with depth. This correlates with the decrease in  $\text{SO}_4^{2-}$  concentrations. Anhydrite is near saturation in the Zeck well, zone 1. For anhydrite the effect of pressure on the mineral solubility was computed both by the empirical function given by Langmuir and Melchior (1985), and using

Table 18. Carbonate mineral saturation indices assuming calcite saturation.

	Sawyer well zone						
	<u>1</u>	<u>2</u>	<u>3</u>	<u>4</u>	<u>5</u>		
dolomite	-0.35	-0.29	-0.32	-0.33	+0.06		
strontianite	-1.22	-1.17	-1.19	-1.20	-1.43		
witherite	-	-	-	-4.90	-5.47		
RaCO <sub>3</sub>	-	-	-	-12.03	-10.95		
	Mansfield well zone		Zeeck well zone				
	<u>1</u>	<u>2</u>	<u>1</u>	<u>2</u>	<u>3</u>		
dolomite	-0.07	-0.12	-0.09	-0.17	+0.07		
strontianite	-1.47	-1.53	-0.63	-1.10	-1.45		
witherite	-5.62	-5.26	-	-	-6.50		
RaCO <sub>3</sub>	-11.53	-11.68	-	-	-11.30		
	J. Friemel well zone						
	<u>1</u>	<u>2</u>	<u>3</u>	<u>4</u>	<u>5</u>	<u>6</u>	<u>7</u>
dolomite	-0.05	-0.05	-0.06	-0.01	+0.02	+0.07	-0.01
strontianite	-1.23	-1.22	-1.26	-1.27	-1.23	-1.24	-1.44

the partial molar volume/compressibility method (cf. Millero, 1982). The empirical function gave results slightly closer to saturation in the lower depths of the J. Friemel well.

Finally, celestite was near saturation in the majority of the samples. The exceptions were the Sawyer well, zones 1-3, the Mansfield well, and the Zeack well, zone 1, where it is undersaturated.

### Conclusions

Sulfate concentrations decrease with depth, probably indicating sulfate reduction is occurring. Increasing concentrations of strontium with depth may be a result of release from a strontium sulfate phase or from a solid solution in gypsum or anhydrite. The saturation state of the sulfate and carbonate minerals was examined using Jenne's "rule of thumb" that a natural water is saturated with respect to a certain mineral if its log IAP is within 1/20 of its log  $K_{sp}$  (Jenne et al., 1980). The sulfate minerals are all saturated in the Palo Duro brines with the exception of  $RaSO_4$  which is significantly undersaturated in all the brines and  $BaSO_4$  in Zeack zone 3. Langmuir and Melchior (1984) related the  $RaSO_4$  undersaturation to the possible formation of a radium solid solution in barite or

celestite. Also, they suggested that the undersaturation of barite in the Zeeck well was a consequence of sulfate reduction. The results presented here and by Langmuir and Melchior (1985) suggest that sulfate minerals may attenuate concentrations of radioactive strontium and radium in the event of their release due to a repository breach.

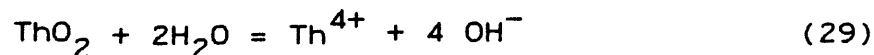
The lack of quality in the carbonate data does not allow direct interpretation of the saturation state of the carbonate minerals as given in Table 17. However, using the assumption of calcite equilibrium, the waters are shown to be also at equilibrium with dolomite, but no other carbonate minerals. Strontianite shows a constant level of undersaturation which may indicate solid solution control over strontium concentrations. Both witherite and  $\text{RaSO}_4$  are greatly undersaturated in the Palo Duro brines. These results indicate that despite the fact that the major lithology is primarily carbonate, the carbonate minerals are too soluble to attenuate introduced radionuclides. The possible exception is  $^{90}\text{Sr}$ , which may be limited by its precipitation in carbonate solid solutions.

ThO<sub>2</sub> AND UO<sub>2</sub> SOLUBILITY STUDYIntroduction

A goal of this research was to study the solubility of thorianite and uraninite in brines, since thorium and uranium both are present in high level nuclear wastes. Further, it has been hypothesized that solubility of their oxides may control concentrations of these elements in the Palo Duro brines.

Thorium is stable only as Th(IV) species under aqueous environmental conditions. In contrast, uranium may exist in the IV, V, or VI state depending upon the pH and system redox potential. The aqueous chemical behavior of Th(IV) measured under ambient oxidizing conditions in the laboratory is similar to that of U(IV) and can therefore be used as an analog for modelling U(IV) behavior in the reduced brines.

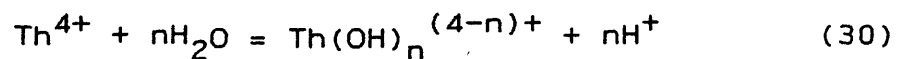
The most stable solid thorium phase is the very insoluble oxide, ThO<sub>2</sub> (thorianite), the dissolution of ThO<sub>2</sub> may be written



At 25°C,  $K_{sp} = 10^{-46.6}$  for amorphous ThO<sub>2</sub> (Langmuir and

Herman, 1980). Based on solubility measurements for a more crystalline phase, Baes and Mesmer (1976) calculated  $K_{sp} = 10^{-49.7}$ . A  $K_{sp}$  of  $10^{-54.2}$  was calculated from the Gibbs free energy of formation from CODATA (1977) which has probably been computed from calorimetric entropy and enthalpy data for a well-crystallized  $\text{ThO}_2$  solid. This difference of -7.6 units in  $\log K_{sp}$  (+10.4 kcal/mol) between the well-crystallized and amorphous oxides is not unreasonable, and is consistent with the low solubility and high nucleation energy of the crystalline oxide.

In the absence of strong complexing agents (ie. organic ligands) the behavior of  $\text{Th}^{4+}$  in dilute aqueous solutions is controlled by hydrolysis reactions which can be represented by the general equation



where  $n = 1$  to  $4$ . Thorium complexing with other inorganic anions is important at low pH and high ionic strength. For this study thorium complexes formed with  $\text{Cl}^-$  and  $\text{SO}_4^{2-}$  were considered. The cumulative formation constants as reported by Langmuir and Herman (1980) are listed in Table 19.

Table 19. Cumulative formation constants at 25°C for mononuclear thorium aquo-complexes. Thorium-hydroxide complexes are written in the proton form (Langmuir and Herman, 1980).

Complex	-log K
$\text{ThOH}^{3+}$	3.2
$\text{Th}(\text{OH})_2^{2+}$	6.9
$\text{Th}(\text{OH})_3^+$	11.7
$\text{Th}(\text{OH})_4^{\circ}$	15.9
$\text{ThCl}^{3+}$	1.09
$\text{Th}(\text{Cl})_2^{2+}$	0.80
$\text{Th}(\text{Cl})_3^+$	1.65
$\text{Th}(\text{Cl})_4^{\circ}$	1.26
$\text{ThSO}_4^{2+}$	5.45
$\text{Th}(\text{SO}_4)_2^{2+}$	9.73

Previous ThO<sub>2</sub> solubility work

There have been few measurements of ThO<sub>2</sub> solubility in aqueous solutions. A summation of the thermodynamic data on the formation of thorium complexes and the dissolution of ThO<sub>2</sub> is given by Langmuir and Herman (1980). The data pertinent to this discussion are given in Table 20. Pitzer (1979) reports interaction coefficients for Th<sup>4+</sup> which he derived from the isopiestic work on ThCl<sub>4</sub> in acidic solutions by Robinson (1955). The solubility of ThO<sub>2</sub> was measured at 95°C and pH < 3 by Baes et al. (1965) who found that equilibrium was attained in 10 days at pH > 2. ThO<sub>2</sub> was precipitated under hydrothermal conditions (< 100°C) from Th(NO<sub>3</sub>)<sub>2</sub> solutions by Robins(1967). None of these studies have considered the effect of ionic strength on the solubility of ThO<sub>2</sub> for intermediate pHs. At intermediate pH's (>5.5) , throughout the ionic strength range of interest (0-4 m NaCl), the predominant thorium aquo species is Th(OH)<sub>4</sub><sup>0</sup>. At high ionic strengths and low pH, Th(Cl)<sub>4</sub><sup>0</sup> is important. The activity coefficients of Th(OH)<sub>4</sub><sup>0</sup> and Th(Cl)<sub>4</sub><sup>0</sup> increase and their molal concentrations decrease as I increases. This behavior is known as salting out, and can be modeled by either a Setchnow equation or by a neutral species Pitzer coefficient.

Table 20. Thermodynamic data for  $\text{ThO}_2$  and thorium aqueous species at  $25^\circ\text{C}$  and 1 atm. <sup>2</sup> pressure from Langmuir and Herman (1980).

Mineral or aqueous species	$\Delta H_f^\circ$	$\Delta G_f^\circ$	$S^\circ$
$\text{ThO}_2(\text{c})$ thorianite	-293.12	-279.35	15.59
$\text{Th}^{4+}$	-183.8	-168.4	-101
$\text{ThOH}^{3+}$	-246.2	-220.7	-79
$\text{Th}(\text{OH})_2^{2+}$	-306.5	-272.3	-53
$\text{Th}(\text{OH})_3^+$	-368.4	-322.5	-36
$\text{Th}(\text{OH})_4^\circ$	-438.4	-373.5	-24
$\text{ThCl}^{3+}$	-223.7	-201.3	-83
$\text{Th}(\text{Cl})_2^{2+}$	-	-232.3	-
$\text{Th}(\text{Cl})_3^+$	-	-264.8	-
$\text{Th}(\text{Cl})_4^\circ$	-	-294.6	-
$\text{ThSO}_4^{2+}$	-397.2	-353.8	-59
$\text{Th}(\text{SO}_4)_2^\circ$	-611.0	-537.6	-22

### Modelling of thorium complexes in brines

To predict the solubility of  $\text{ThO}_2$  in brines it is necessary to determine how increasing ionic strength affects the activities of dissolved thorium species including, complexes. This requires data on the variation of activity coefficients for  $\text{Th}^{4+}$  and Th complexes with ionic strength that can be input into an ion-interaction computer code. Such data exist for  $\text{Th}^{4+}$  in acidic chloride solutions. Lacking ion-interaction parameters for the thorium hydroxy, chloride and sulfate complexes, the best option is to assume that they equal the measured parameters for species of comparable size and identical charge. Accordingly, for  $\text{Th}(\text{OH})_3^+$  and  $\text{Th}(\text{Cl})_3^+$  the analog chosen was  $\text{Cs}^+$ . For  $\text{Th}(\text{OH})_2^{2+}$ ,  $\text{Th}(\text{Cl})_2^{2+}$  and  $\text{ThSO}_4^{2+}$  the analog species was  $\text{Ba}^{2+}$ . For  $\text{ThOH}^{3+}$  and  $\text{ThCl}^{3+}$  the analog chosen was  $\text{La}^{3+}$ . Values of the parameters for these species and for  $\text{Th}^{4+}$  were obtained from Pitzer (1987). For the neutral complexes  $\text{Th}(\text{OH})_4^0$ ,  $\text{Th}(\text{Cl})_4^0$  and  $\text{Th}(\text{SO}_4)_2^0$ , the analog chosen was  $\text{Si}(\text{OH})_4^0$  ( $\text{H}_4\text{SiO}_4$ ). The activity coefficient of a neutral species can be given by

$$\log \gamma = Dm \quad (31)$$

where the value of D, the empirical Setchenow constant, is a

function of the nature of the electrolyte and  $m$  is the molality of the electrolyte. Values of  $D$  for silica in various salt solutions are given by Marshall and Chen (1982). For the NaCl system  $D = 0.0803$  at  $25^{\circ}\text{C}$ . Using the assumption  $D(\text{K}^+) = D(\text{Cl}^-)$  the neutral interaction terms ( $L$ ) used to model neutral species activities in the ion-interaction equations are  $L_{\text{Na}} = -0.033$  and  $L_{\text{Cl}} = 0.007$ .

Previous workers have also used analog species to proxy for other species when appropriate electrolyte data were lacking. Thus, Pitzer (1979) suggested the use of  $\text{Mg}^{2+}$  as an analog for  $\text{Ca}^{2+}$ . The use of other alkaline-earth elements (Ca, Ba, Sr) as analog for each other (Rogers, 1981) and for radium (Langmuir and Melchior, 1985) has proven successful for modeling the behavior of  $\text{SrSO}_4$ ,  $\text{BaSO}_4$ , and  $\text{RaSO}_4$  in brines.

Table 21 summarizes the ion-interaction parameters needed to model the activities of aqueous thorium species in NaCl solutions as a function of pH and ionic strength. Model computed activities of thorium species in a series of NaCl brines are given in Table 22.

Once activities of the thorium aqueous species have been calculated using the Pitzer equations, and with the various complex formation constants, it is possible to generate a series of stability diagrams showing the mole

Table 21. Pitzer ion-interaction parameters for the thorium species in NaCl solutions at 25°C.

Species	Analog	$\beta^{\circ}$	$\beta^{\circ}$	$C^{\circ}$	$\phi$	$\psi$
Th <sup>4+</sup>	-	1.0138	13.3313	-0.1034	0.0	0.0
ThOH <sup>3+</sup>	La <sup>3+</sup>	0.58867	5.60	-0.02348	0.0	0.0
Th(OH) <sub>2</sub> <sup>2+</sup>	Ba <sup>2+</sup>	0.2628	1.4963	-0.01938	0.7	-0.007
Th(OH) <sub>3</sub> <sup>+</sup>	Cs <sup>+</sup>	0.030	0.0558	0.00038	0.033	-0.003

Table 22. Model computed activity coefficients of thorium species in NaCl media at 25°C using analogous species.

I (m)	Th <sup>4+</sup>	ThOH <sup>3+</sup>	Th(OH) <sub>2</sub> <sup>2+</sup>	Th(OH) <sub>3</sub> <sup>+</sup>	Th(OH) <sub>4</sub> <sup>0</sup>
		ThCl <sup>3+</sup>	Th(Cl) <sub>2</sub> <sup>2+</sup>	Th(Cl) <sub>3</sub> <sup>+</sup>	Th(Cl) <sub>4</sub> <sup>0</sup>
			ThSO <sub>4</sub> <sup>2+</sup>		Th(SO <sub>4</sub> ) <sub>2</sub> <sup>0</sup>
0.005	0.233	0.469	0.729	0.924	1.00
0.010	0.138	0.357	0.650	0.896	1.00
0.050	0.0246	0.142	0.438	0.800	1.01
0.100	0.0101	0.0869	0.351	0.742	1.02
0.250	3.11×10 <sup>-3</sup>	0.0444	0.257	0.653	1.05
0.500	1.37×10 <sup>-3</sup>	0.0275	0.208	0.577	1.09
0.750	8.45×10 <sup>-4</sup>	0.0213	0.188	0.531	1.14
1.00	5.87×10 <sup>-4</sup>	0.0178	0.179	0.497	1.20
1.50	3.29×10 <sup>-4</sup>	0.0142	0.174	0.449	1.31
2.0	2.06×10 <sup>-5</sup>	0.0124	0.178	0.415	1.43
3.0	9.86×10 <sup>-6</sup>	0.0112	0.201	0.367	1.71
4.0	5.69×10 <sup>-6</sup>	0.0115	0.237	0.332	2.05
5.0	6.95×10 <sup>-6</sup>	0.0209	0.302	0.294	2.45

fraction abundance of each species. Thorium-hydroxy and thorium-chloride complex distribution diagrams were prepared assuming total thorium concentrations  $<10^{-5}$  m for which conditions Th is present only as mononuclear species (cf. Baes and Mesmer, 1976), and the pH distribution of complexes is independent of total thorium concentration. The cumulative formation constants taken from Table 19 were used along with activity coefficients for the thorium species from Table 22 in a calculation scheme outlined in Butler (1964, pp. 267-268). A program to perform the calculations was written in BASIC and executed on an IBM-PC. Figures 3-7 present the distribution diagrams for the Th aquo-species at ionic strengths of 0.1, 0.5, 1.0 and 4.0 molal in NaCl media at 25°C.

The distribution diagrams show that with increasing ionic strength the importance of thorium-chloride complexes increases at the expense of  $\text{Th}^{4+}$  and the intermediate thorium-hydroxy complexes. Thus for  $I = 4.0$  m,  $\text{Th}(\text{Cl})_4^0$  and  $\text{Th}(\text{OH})_4^0$  are the predominant species in NaCl media. These results indicate that in high ionic strength NaCl solutions, the distribution of thorium complexes is independent of pH except in the 5 to 6 range. Having predicted the relative behavior of thorium hydroxy complexes as a function of ionic strength we can relate these results to the measured

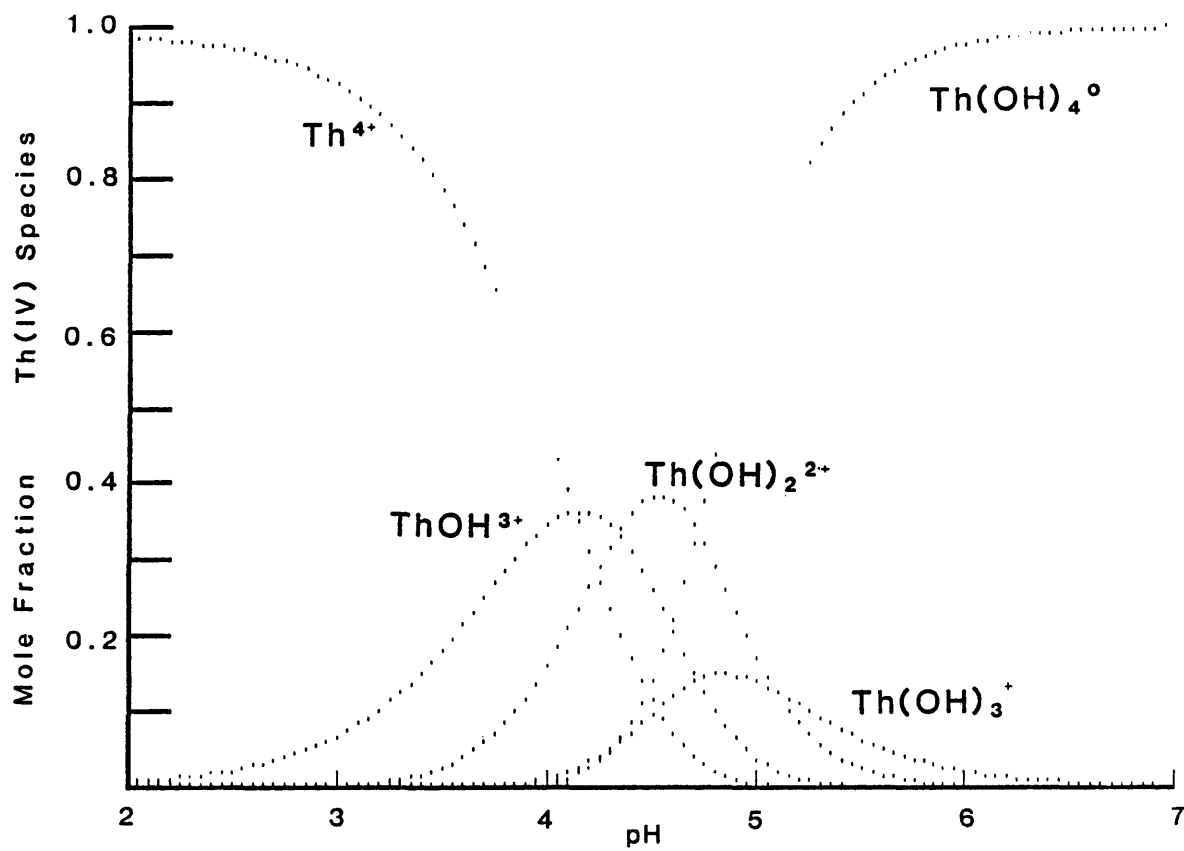


Figure 3. Distribution of  $\text{Th}^{4+}$  and Th-aquo complexes as a function of pH in 0.1 m NaCl at 25°C.

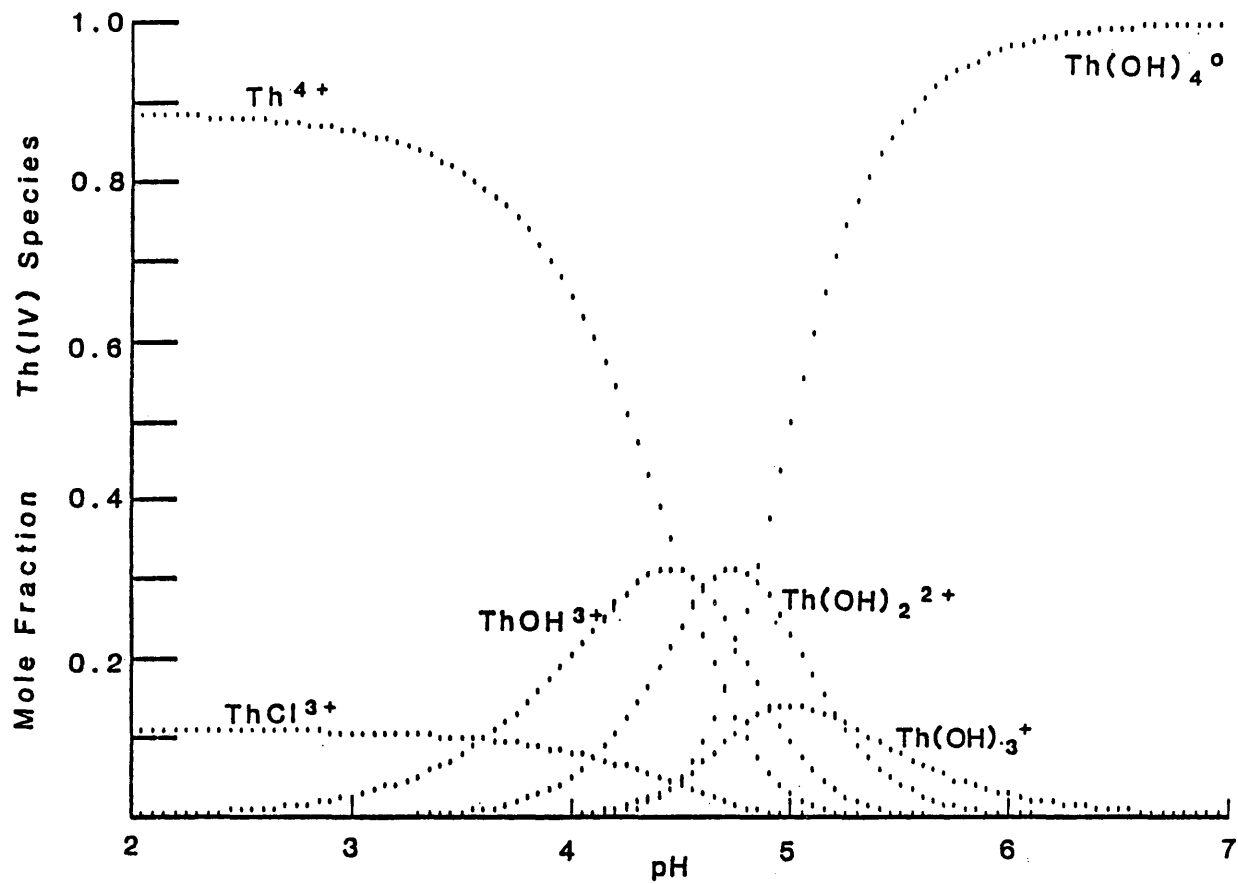


Figure 4. Distribution of  $\text{Th}^{4+}$  and Th-aquo complexes as a function of pH in 0.5 molal NaCl at 25°C.

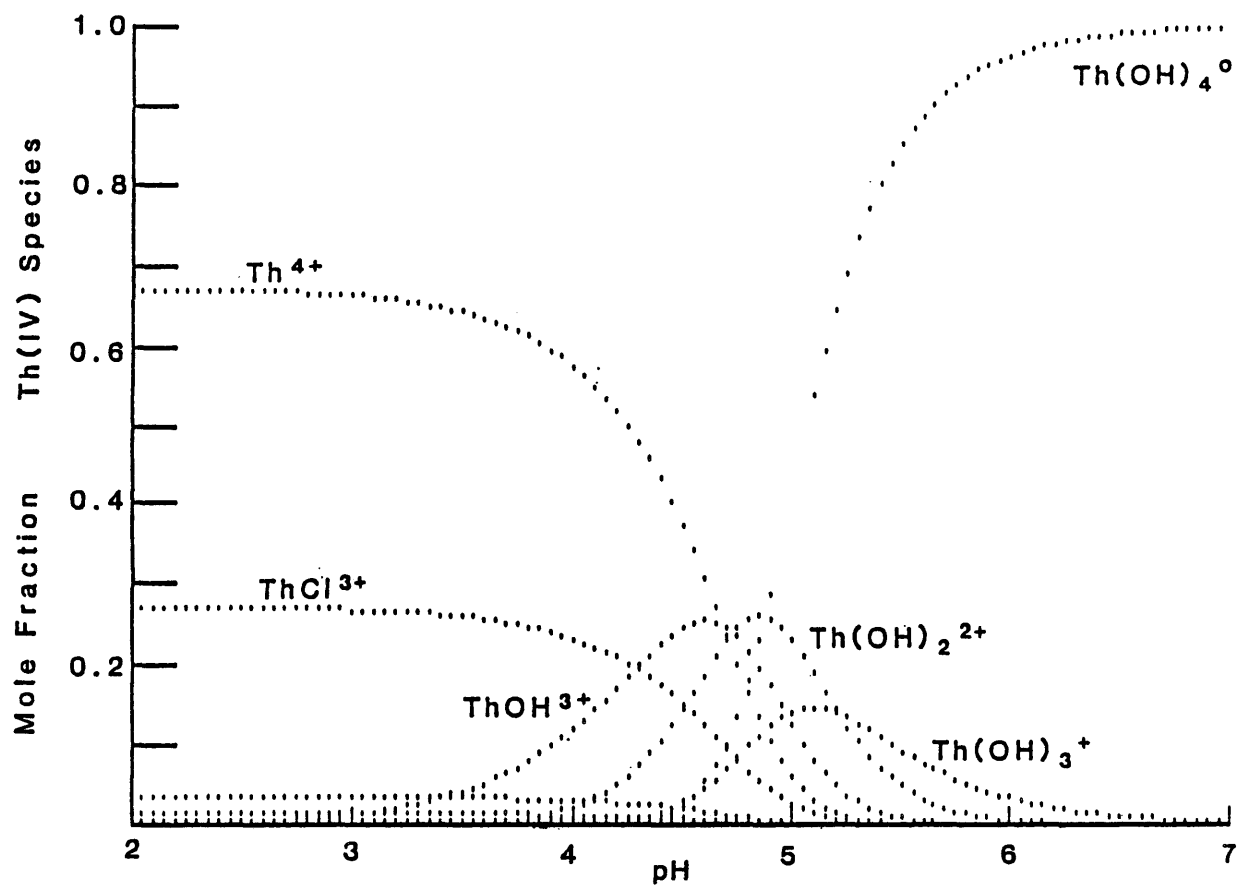


Figure 5. Distribution of  $\text{Th}^{4+}$  and Th-aquo complexes as a function of pH in 1.0 molal NaCl at 25°C.

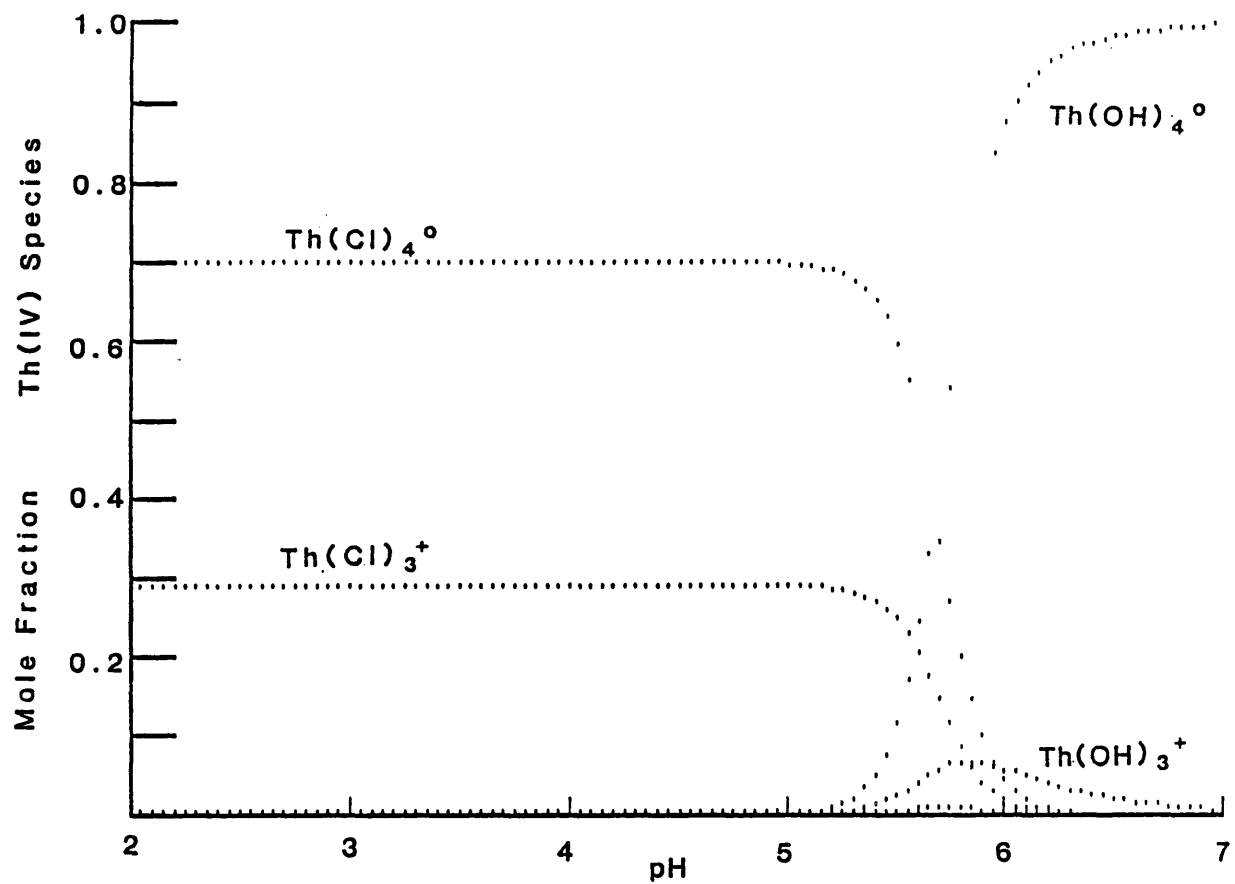


Figure 6. Distribution of  $\text{Th}^{4+}$  and Th-aquo complexes as a function of pH in 4.0 molal NaCl at 25°C.

solubility of  $\text{ThO}_2$  in NaCl solutions.

### Experimental

A series of experiments were performed to measure the solubility of  $\text{ThO}_2$  in NaCl solutions ranging in ionic strength from 0.0 to 4.0 molal. Prior to the solubility runs, reagent grade or better  $\text{ThO}_2$  solid was ultrasonically dispersed in water and allowed to settle briefly. The suspension was decanted to remove the suspended fine particles which have a higher solubility due to surface energy effects. The remaining solid material was dried at  $110^\circ\text{C}$  for two days then stored in a glass vial with a tight fitting screw cap.

For the solubility runs, small quantities of  $\text{ThO}_2$  (200-900 ug) were weighed out on an CAHN microbalance and placed in 1-liter linear polyethylene bottles (LPE). Prior to their use, the bottles were washed with Alconox detergent and rinsed several times with doubly-deionized water. Weighed quantities of reagent grade NaCl were added to each bottle. One liter of doubly deionized water was added to the salt and the bottles sealed with tightly-fitting screw caps and placed in a shaking constant temperature bath. The samples were agitated throughout the experiment and the temperature maintained to  $\pm 0.1^\circ\text{C}$ . The experiments were

performed at 35°C in an attempt to increase the kinetics of dissolution. Solubility experiments must be performed from both under- and super-saturation in order to assure attainment of equilibrium. To facilitate this, one set of experiments was maintained at 45°C for the first half of the experiment and then lowered to 35°C for the remainder of the experiment. A second set of experiments were maintained at 35°C throughout. Total length of the solubility runs were approximately eight months.

At the conclusion of experiments sample pH's were measured with a Beckman micropore combination pH electrode and an Orion 901 meter. The electrode was standardized using pH 4.01 and 6.86 Fisher gram-pac buffers. The samples were centrifuged at 2500 rpm for 45 minutes in the LPE bottles in order to settle any fine particles. The upper one half of the sample (500 ml) was then siphoned into a new LPE bottle and acidified to pH < 2 using ultrex nitric acid. The samples were then sent to Pacific Northwest Labs for  $^{232}\text{Th}$  and  $^{228}\text{Th}$  analysis by alpha counting. The analyses were performed by Dr. J.C. Laul.

### Experimental results

Total molal concentrations of thorium computed from the radioactive decay rate of  $^{232}\text{Th}$  are given in Table 23.

Table 23. Molal concentrations of  $^{232}\text{Th}$  and final pHs in NaCl solutions at  $35^\circ\text{C}$ . Uncertainties are based on alpha counting errors.

I (m)	Sample L		Sample H	
	mTh( $\times 10^{11}$ )	pH	mTh( $\times 10^{11}$ )	pH
0.0	9.54 $\pm$ 3.53	5.29	24.73 $\pm$ 7.07	5.56
0.005	6.71 $\pm$ 3.53	5.49	21.20 $\pm$ 12.37	5.39
0.010	19.43 $\pm$ 5.30	5.29	19.43 $\pm$ 5.30	5.39
0.050	9.01 $\pm$ 3.53	5.30	28.27 $\pm$ 7.07	5.43
0.10	14.66 $\pm$ 7.07	5.08	83.03 $\pm$ 35.33	5.46
0.25	11.84 $\pm$ 5.30	5.55	24.73 $\pm$ 7.07	5.41
0.50	22.97 $\pm$ 7.07	6.31	12.37 $\pm$ 5.30	5.71
0.75	14.13 $\pm$ 3.53	5.87	10.60 $\pm$ 3.53	6.37
1.0	8.83 $\pm$ 3.53	5.96	14.84 $\pm$ 5.30	6.26
1.5	54.76 $\pm$ 10.60	6.18	28.27 $\pm$ 8.83	5.63
2.0	2,140 $\pm$ 7.07	6.45	12.37 $\pm$ 3.53	6.20
3.0	40.63 $\pm$ 12.37	6.48	104.23 $\pm$ 17.66	6.60
4.0	388.6 $\pm$ 37.10	6.73	33.56 $\pm$ 12.37	6.21

Examination of the data show two samples labeled L with anomalously high Th values at ionic strengths of 2.0 and 4.0 molal. These values are most likely the result of suspended particulate  $\text{ThO}_2$  not removed by centrifugation or resuspended during the siphoning process. These two data points were rejected. Unfortunately, the remaining data show a great deal of scatter and no systematic trends. The uncertainty introduced by counting (analytical) error seems to be nearly as great as the experimental variation. The considerable variability in Th concentrations is understandable at these very low levels. The scatter in the pH data is more difficult to explain as there should be a clear trend in the pH with increasing ionic strength.

Calculated mole fractions of the thorium complexes show that  $\text{Th}(\text{OH})_4^{\circ}$  is the dominant thorium species in all of the experiments. Given the low precision of the data, one can assume that  $\text{Th}(\text{OH})_4^{\circ}$  is the only species present without introducing significant error.  $\text{ThO}_2$  solubility is then governed by the reaction



If this is correct, then the solubility is pH-independent and proportional to  $10^{-0.078I}$  in NaCl solutions at  $35^{\circ}\text{C}$

(Marshall and Chen, 1982), assuming the silica analog adequately explains  $\text{Th}(\text{OH})_4^{\circ}$  behavior. This behavior would result in a concentration decrease of  $9.3 \times 10^{-11} \text{ m}$  in dissolved thorium between 0.0 and 4.0 m ionic strength. Such a trivial change in the thorium concentration is well within the experimental uncertainty, and cannot be discerned from the empirical data. A value for the equilibrium constant for the above reaction was obtained from the experimental data using the expression

$$K_{\text{sp}} = (\text{mTh}(\text{OH})_4^{\circ})(\gamma\text{Th}(\text{OH})_4^{\circ})/(\text{H}_2\text{O})^2 \quad (33)$$

The values of  $K_{\text{sp}}$  at  $35^{\circ}\text{C}$ , computed assuming that the Setchenow coefficient for silica applies to  $\text{Th}(\text{OH})_4^{\circ}$ , are presented in Table 24. The average  $\log K_{\text{sp}}$  computed from the data is  $-9.58$  with a standard deviation of  $0.40$ . This is in reasonable agreement with the value  $-9.79$  computed from the solubility work summarized by Baes and Mesmer (1976). Values computed using the two rejected data points fall well outside of three standard deviations of the mean, and justified their rejection. Although the experimental data do not prove that the predominant thorium species is  $\text{Th}(\text{OH})_4^{\circ}$  or that the behavior of this species is adequately modelled by silica, the results are in keeping with these

Table 24. Experimentally determined equilibrium constants ( $-\log K$ ) for reaction (32) in NaCl solutions at 35°C.

<u>I(m)</u>	<u>(L)</u>	<u>(H)</u>
0.0	10.02	9.61
0.005	10.17	9.67
0.010	9.70	9.70
0.050	10.03	9.54
0.10	9.81	9.06
0.25	9.88	9.56
0.50	9.57	9.84
0.75	9.75	9.87
1.0	9.91	9.68
1.5	9.06	9.35
2.0	-	9.61
3.0	8.98	8.57
4.0	-	8.94

assumptions (ie. no discernable effect of increasing ionic strength on the concentration of thorium).

The effect of pH, ionic strength, and temperature on ThO<sub>2</sub> solubility

The thorium oxide solubility experiments gave an average  $\log K = -49.5$  for the equilibrium constant of reaction 29 at 35°C. With this constant and the activity coefficients of the thorium complexes from Table 22, we may compute the solubility of ThO<sub>2</sub> as a function of ionic strength and pH. The results are given in Table 25. Table 25 shows that high NaCl salinities greatly increase the solubility of ThO<sub>2</sub> below pH 5, but that at higher pHs, ThO<sub>2</sub> solubility is practically independent of ionic strength and pH.

With the enthalpy data from Table 20, the effect of temperature on ThO<sub>2</sub> solubility was computed. Since enthalpies were not available for the important thorium-chloride complexes, the effect of temperature on ThO<sub>2</sub> solubility could be computed only for the high pH data in the high ionic strength solutions. The results are also given in Table 25. The table shows that an increase in temperature increases ThO<sub>2</sub> solubility below approximately pH 5 and decreases its solubility above approximately pH 5. The

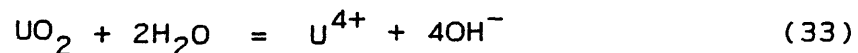
Table 25. Solubility of  $\text{ThO}_2$  expressed as  $-\log m \text{ Th}$  as a function of pH, ionic strength and temperature in NaCl solutions.

T = 25°C		pH				
I	2	3	4	5	6	7
0.01	-0.84	-4.75	-8.03	-9.48	-9.60	-9.60
0.1	+0.29	-3.70	-7.40	-9.44	-9.60	-9.60
0.5	+1.24	-2.76	-6.76	-9.53	-9.64	-9.66
1.0	+1.64	-2.36	-6.30	-9.31	-9.68	-9.69
4.0	+2.24	-1.76	-5.76	-9.76	-10.00	-10.05
T = 35°C						
0.01	-0.24	-4.20	-7.64	-9.54	-9.80	-9.80
4.0	-	-	-	-	-10.20	-10.30
T = 45°C						
0.01	+0.36	-3.59	-7.38	-9.47	-10.0	-10.0
4.0	-	-	-	-	-10.3	-10.5

magnitude of the temperature effect is somewhat greater below pH 5.

The effect of pH, ionic strength, and temperature on UO<sub>2</sub> solubility and U(IV) complexes

Under reducing conditions such as in the Palo Duro brines, UO<sub>2</sub> behaves in a manner similar to ThO<sub>2</sub>, and the results of the ThO<sub>2</sub> solubility study can be used as an analog to predict UO<sub>2</sub> solubility in the brines. The dissolution of crystalline UO<sub>2</sub> (uraninite) below about pH 2 may be written



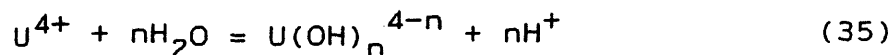
where  $K_{sp} = 10^{-60.6}$  based on Gibbs free energy data from Langmuir (1978). Langmuir (1978) estimated  $K_{sp} = 10^{-55}$  for amorphous UO<sub>2</sub>. Above pH 4 the chief reaction is



where  $K = 10^{-13.2}$  and  $10^{-7.2}$ , for crystalline and amorphous UO<sub>2</sub> respectively, also from Langmuir (1978). Although previous workers (cf. Langmuir, 1978; Lemire and Tremaine, 1980) have proposed a  $\text{U}(\text{OH})_5^-$  complex at higher pH's,

unpublished work by G. Parks of Stanford (1984) casts some doubt on its existence.

As in the thorium system, the behavior of uranium (IV) in NaCl solutions is dominated by hydrolysis reactions of the type



with  $n = 0$  to 4. Cumulative formation constants of the hydroxy complexes as given by Langmuir (1978) are listed in Table 26. Uranium-chloride complexes are also important at low pH in high ionic strength solutions. Unfortunately, data is only available for  $UCl^{3+}$  and  $U(Cl)_2^{2+}$  (Table 26). This limits the rigorous modeling of uranium speciation at low pH in high ionic strength waters.

The effect of ionic strength on the distribution of U(IV) aquo-species and  $UO_2$  solubility in NaCl solutions may be estimated using activity coefficients developed for the thorium system via the analog approach and ion-interaction calculations, combined with equilibrium constants for reactions given above. The results for 25°C are plotted in Figures 7-10 for ionic strengths of 0.1 through 4.0 molal. The chief difference between the uranium and thorium systems is the greater importance of hydroxy complexes and

Table 26. Cumulative formation constants at 25°C for mononuclear uranium aquo-complexes. Uranium-hydroxide complexes written in the proton form (Langmuir, 1978).

Complex	-log K
$\text{UOH}^{3+}$	0.66
$\text{U}(\text{OH})_2^{2+}$	2.3
$\text{U}(\text{OH})_3^+$	4.9
$\text{U}(\text{OH})_4^{\circ}$	8.6
$\text{UCl}^{3+}$	1.0
$\text{U}(\text{Cl})_2^{2+}$	0.25
$\text{USO}_4^{2+}$	5.46
$\text{U}(\text{SO}_4)_2^{\circ}$	9.75

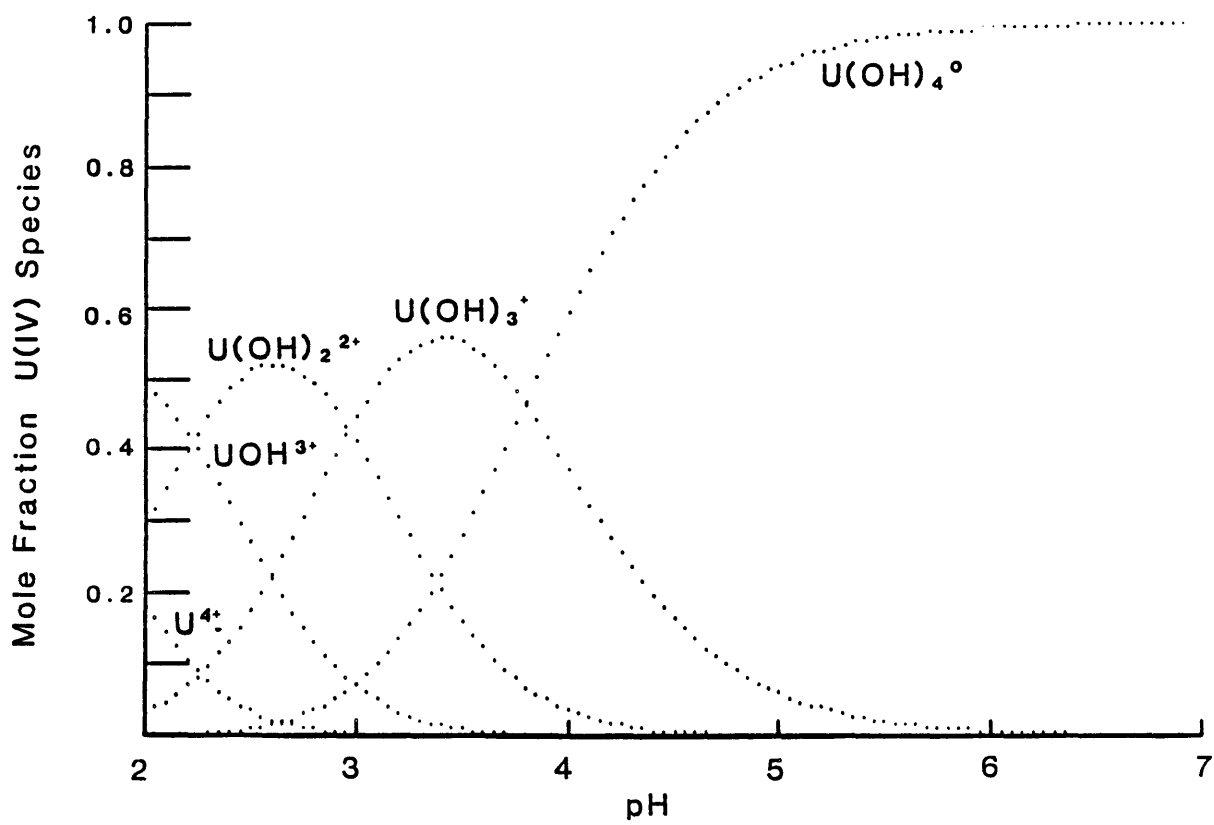


Figure 7. Distribution of  $U^{4+}$  and U-aquo complexes as a function of pH in 0.1 m NaCl at 25°C.

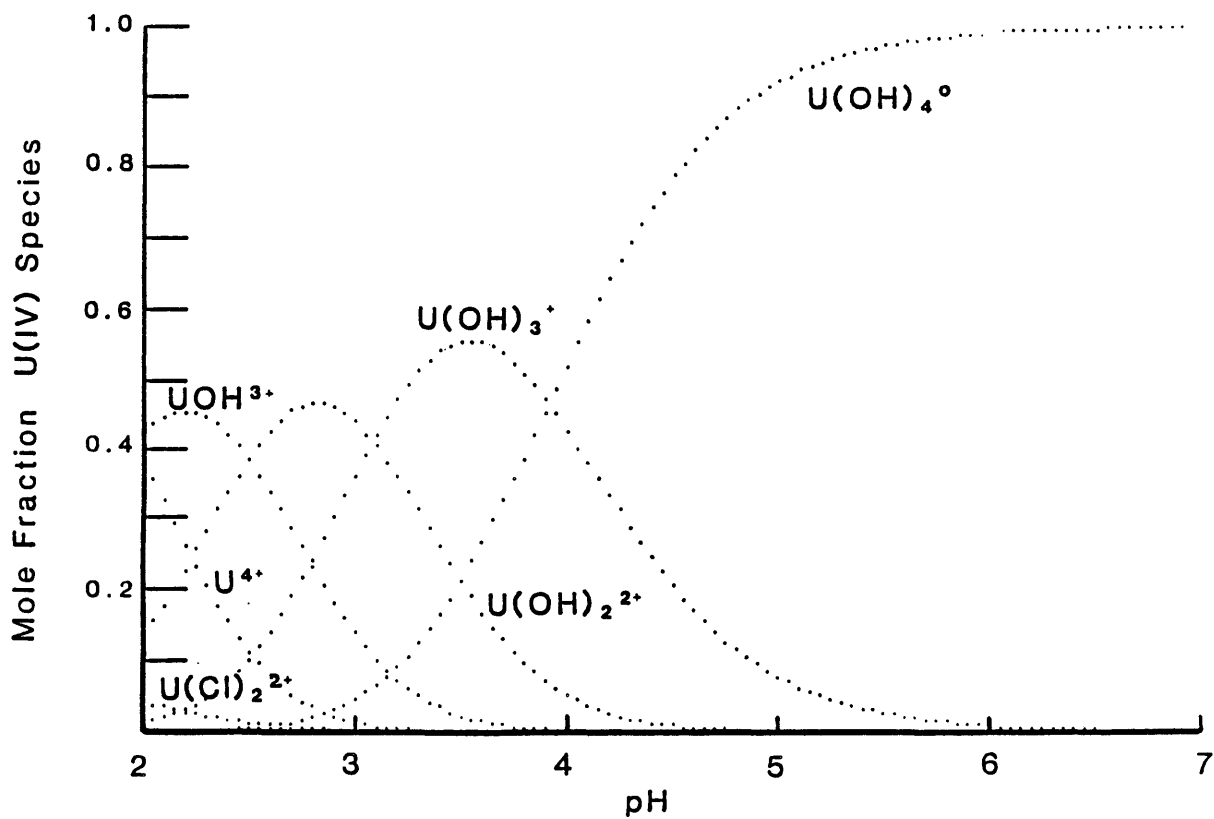


Figure 8. Distribution of  $U^{4+}$  and U-aquo complexes as a function of pH in 0.5 molal NaCl at 25°C.

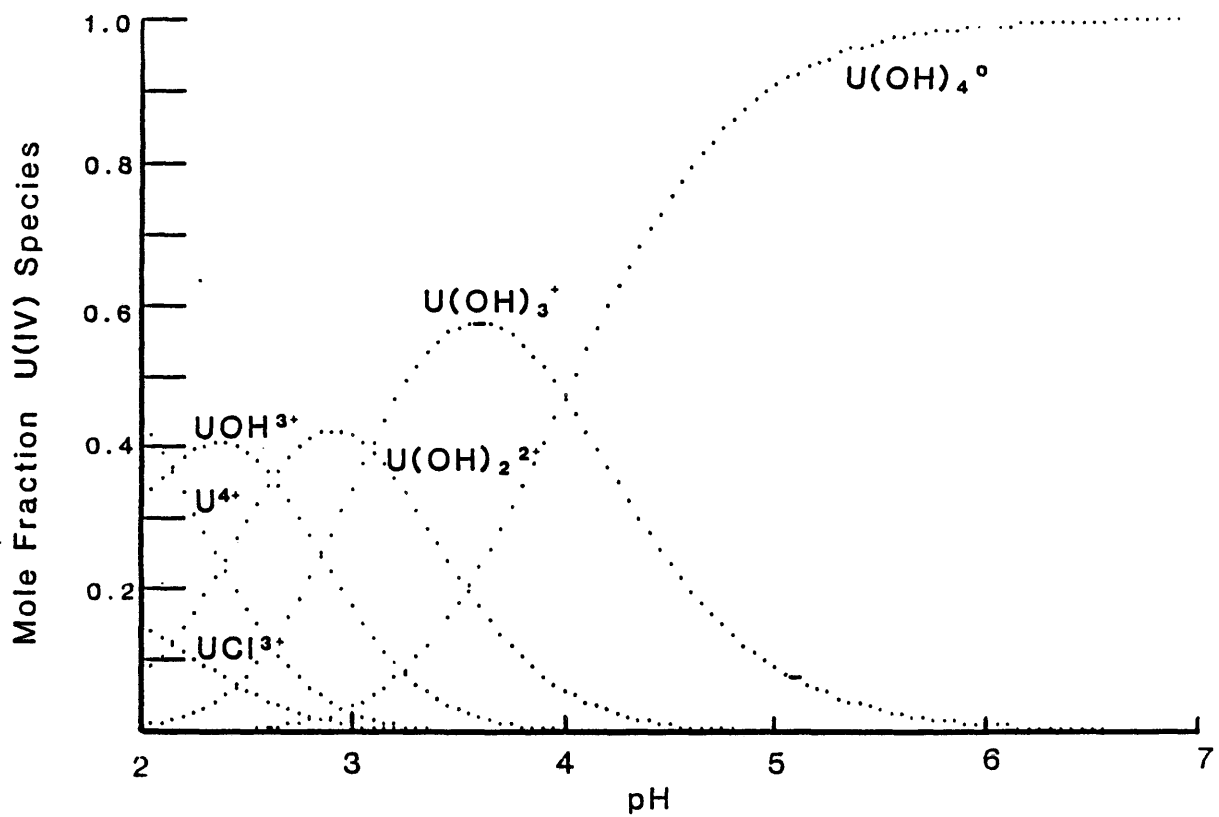


Figure 9. Distribution of U<sup>4+</sup> and U-aquo complexes as a function of pH in 1.0 molal NaCl at 25°C.

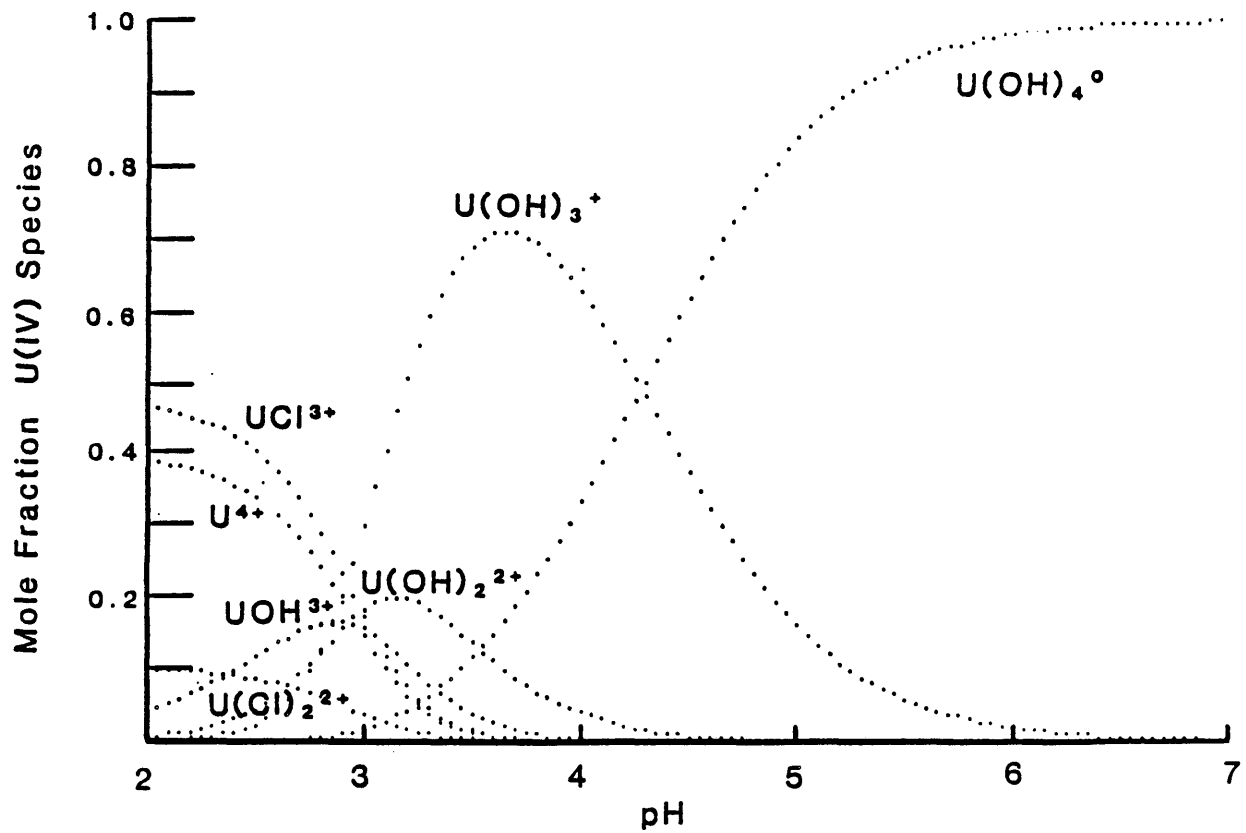


Figure 10. Distribution of  $U^{4+}$  and U-aquo complexes as a function of pH in 4.0 molal NaCl at 25°C.

lesser importance of chloride complexes in the uranium system. The solubility of  $UO_2$  as a function of temperature between 25 and 45°C may be computed with enthalpy data from Langmuir (1978) and the van't Hoff equation. The enthalpies of reactions 33 and 34 are +34.7 kcal/mol and +6.13 kcal/mol, respectively. The enthalpy for the formation of  $UCl_3^+$  is +9.93 kcal/mol. Figure 11 shows the results of the solubility calculations as a function of pH, ionic strength and temperature. Solubility is relatively independent of all three variables above pH = 5.

#### ThO<sub>2</sub> and UO<sub>2</sub> solubility in the Palo Duro brines

Using the results of the ThO<sub>2</sub> solubility measurements in NaCl solutions, and the model calculations for ThO<sub>2</sub> and UO<sub>2</sub> solubilities as a function of pH, ionic strength and temperature, we can make a preliminary assessment of the solubility of thorium and uranium in the Palo Duro brines. No data is currently available on the effect of pressure on ThO<sub>2</sub> and UO<sub>2</sub> solubility, so it was necessary to ignore this effect. The concentrations of thorium and uranium have been measured by Laul et al. (1984) in four Palo Duro brines, and are presented in Table 27. Using procedures described above, and the equilibrium constants for the various inorganic complexes from Tables 19 and 26, the distribution of aquo

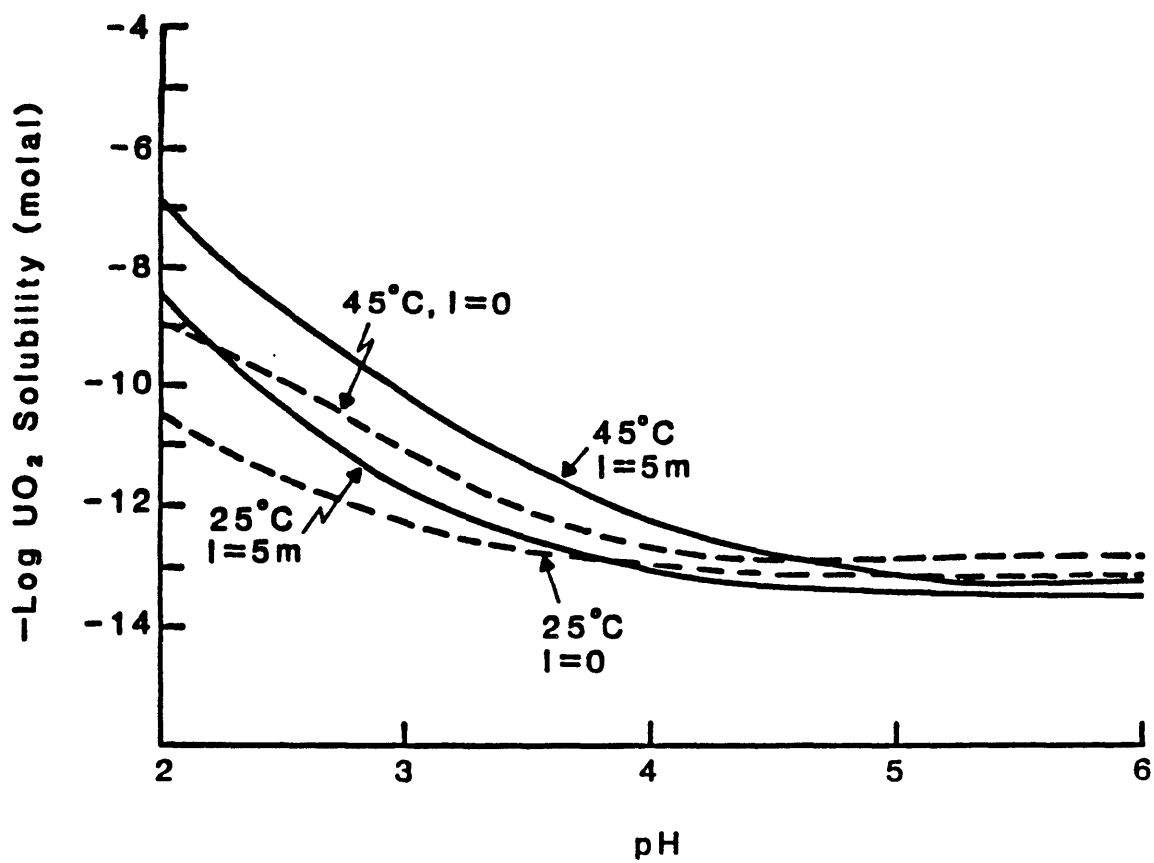


Figure 11. Effect of pH, ionic strength and temperature on the solubility of crystalline  $\text{UO}_2$  predicted by the Pitzer ion-interaction model.

Table 27. Molal concentrations of thorium and uranium in some Palo Duro brines as reported by Lau1 et al. (1984)

Brine sample	Th	U
Sawyer, zone 4	$2.6 \times 10^{-10}$	$1.5 \times 10^{-9}$
Sawyer, zone 5	$5.26 \times 10^{-9}$	$1.4 \times 10^{-9}$
Mansfield, zone 1	$2.2 \times 10^{-10}$	$9.2 \times 10^{-10}$
Mansfield, zone 2	$3.5 \times 10^{-10}$	$6.7 \times 10^{-10}$

complexes can be computed. Additionally, the importance of organic complexes must be evaluated. The major component of the TOC (total organic carbon) in the Palo Duro brines is acetate, which ranges from 7 to 101 mg/l (Means, 1986). The formation constant for the thorium acetate complex is  $10^{3.9}$  (Martell and Smith, 1977). Assuming an equal value for the formation constant of the  $U^{4+}$ -acetate complex, we may compute that neither complex is important in the Palo Duro brines. The distribution of thorium complexes in the Palo Duro brines are:

Sawyer well, zone 4: 64%  $Th(Cl)_4^{\circ}$  and 36%  $Th(Cl)_3^{+}$

Sawyer well, zone 5: 100%  $Th(OH)_4^{\circ}$

Mansfield well, zone 1: 100%  $Th(OH)_4^{\circ}$

Mansfield well, zone 2: 41%  $Th(Cl)_4^{\circ}$ , 27%  $Th(Cl)_3^{+}$ , 24%  $Th(OH)_4^{\circ}$  and 8%  $Th(SO_4)_2^{\circ}$ .

For uranium the distributions are:

Sawyer well, zone 4: 100%  $U(OH)_4^{\circ}$

Sawyer well, zone 5: 100%  $U(OH)_4^{\circ}$

Mansfield well, zone 1: 100%  $U(OH)_4^{\circ}$

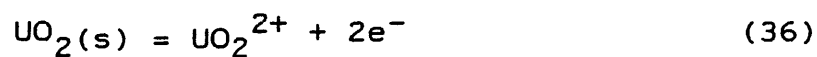
Mansfield well, zone 2: 93%  $U(OH)_4^{\circ}$  and 7%  $U(OH)_3^{+}$

Assuming the above complexing, theoretical concentrations of thorium and uranium at equilibrium with the crystalline and amorphous oxides was calculated. The results are given in Table 28. The results of the

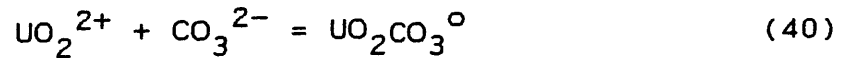
Table 28. Predicted and measured  $-\log$  molal solubilities of crystalline (c) and amorphous (am)  $\text{ThO}_2$  and  $\text{UO}_2$  in some Palo Duro brines.

Brine sample	$-\log$ (m Th)			$-\log$ (m U)		
	measured	predicted (c) (am)		measured	predicted (c) (am)	
Sawyer, zone 4	8.3	7.7 4.6		8.7	13.7 8.1	
Sawyer, zone 5	9.6	9.9 6.8		8.8	13.5 7.9	
Mansfield, zone 1	9.6	10.1 7.0		8.8	13.7 8.1	
Mansfield, zone 2	9.5	8.4 5.1		9.0	13.7 8.1	

calculations for thorium solubility indicate  $\text{ThO}_2$  is near saturation in the Palo Duro brines. However the Mansfield well, zone 2 is somewhat undersaturated ( $\text{SI} = -1.3$ ), possibly indicating a sorption control. The results indicate the mobility of thorium, introduced by a repository breach, will be limited by  $\text{ThO}_2$  solubility. Amorphous  $\text{UO}_2$  appears to be at saturation in the Palo Duro brines. However, due to the extreme age of the sediments and the ground waters, a more crystalline  $\text{UO}_2$  phase would be expected to control uranium solubility. The simplest explanation is that some or all of the dissolved uranium is present as U(VI). Under the pH conditions of the Palo Duro basin ( $\text{pH} < 6.5$ ) the forms of U(IV) are  $\text{UO}_2^{2+}$  and  $\text{UO}_2\text{CO}_3^0$ . Eh has a profound effect on the solubility of  $\text{UO}_2$ . However no Eh data is available for this system so it is not possible to determine the redox state of uranium directly. Noticable  $\text{H}_2\text{S}$  odors from some of the brines would indicate the Eh is within 0.1 volts of the  $\text{H}_2\text{S}-\text{SO}_4$  boundary. The measured total uranium concentration is assumed to be the sum of  $\text{U}(\text{OH})_4^0$ ,  $\text{UO}_2^{2+}$  and  $\text{UO}_2\text{CO}_3^0$ . The activity coefficient for the uranyl-carbonate complex was determined assuming  $\gamma_{\text{UO}_2\text{CO}_3^0} = \gamma_{\text{H}_4\text{SiO}_4^0}$ . Using the reactions



with  $E^{\circ} = + 0.260 \pm 0.003$  volts (Bruno et al., 1985) and



with  $K = 10^{10.1}$ , an Eh can be computed for  $\text{UO}_2$  saturation. Calculated Eh's (volts) assuming crystalline  $\text{UO}_2$  saturation are: Sawyer well, zone 4, +0.09; Sawyer well, zone 5, +0.06; and Mansfield well, zones 1 and 2, +0.07. In the absence of measured Eh or uranium speciation, it is not possible to state whether  $\text{UO}_2$  solubility would limit uranium concentrations in the Palo Duro brines should a repository breach occur.

REFERENCES CITED

- Atwood, H. and Pickering, L. 1986. A preliminary simulation model to determine ground-water flow and ages within the Palo Duro hydrogeologic province. *in* Symposium on groundwater flow and transport modeling for performance assessment of deep geologic disposal of radioactive waste; a critical evaluation of the state of the art. Proceedings. May 20-21, 1985. Albuquerque, NM.
- Baes, C.F. and Mesmer, R.E. 1976. *The Hydrolysis of Cations*. Wiley-Interscience, New York, NY. 496pp.
- Baes, C.F., Meyer, N.J. and Roberts, C.E. 1965. The hydrolysis of thorium(IV) at 0 and 95 C. *Inorg. Chem.* 4:518-527.
- Bassett, R.L. and Bently, M.E. 1982. Geochemistry and hydrodynamics of deep formation brines in the Palo Duro and Dalhart basins, Texas, U.S.A. *J. of Hydrol.* 59:331-372.
- Basset, R.L. and Bently, M.E. 1983. Deep brine aquifers in the Palo Duro basin: Regional flow and geochemical constraints. *Texas Bur. Econ. Geol. Report of Investigations. no. 130*, 59pp.
- Bates, R.G. 1973. *Determination of pH. Theory and Practice*. 2nd Ed. John Wiley and Sons, New York, N.Y. 479pp.
- Blount, C.W. 1977. Barite solubilities and thermodynamic quantities up to 300°C and 1400 bars. *Amer. Mineral.* 62: 942-957.
- Blount, C.W. and Dickson, F.W. 1973. Gypsum-anhydrite equilibria in systems  $\text{CaSO}_4\text{-H}_2\text{O}$  and  $\text{CaSO}_4\text{-NaCl-H}_2\text{O}$ . *Amer. Mineral.* 58:323-331.
- Bruno, J., Grenthe, I. and Lagerman, B. 1985. Redox processes and  $\text{UO}_2(\text{s})$  solubility: The determination of the  $\text{UO}_2^{2+}/\text{U}^{4+}$  redox potential at 25°C in  $\text{HClO}_4$  media of different strength. *Mat. Res. Soc. Symp. Proc.* 50:299-308.

Busenberg, E., Plummer, L.N. and Parker, V.B. 1984. The solubility of strontianite ( $\text{SrCO}_3$ ) in  $\text{CO}_2$ - $\text{H}_2\text{O}$  solutions between 2 and 91°C, the association constants of  $\text{SrHCO}_3^+$ (aq) and  $\text{SrCO}_3^0$ (aq) between 5 and 80°C, and an evaluation of the thermodynamic properties of  $\text{Sr}^{2+}$ (aq) and  $\text{SrCO}_3$ (cr) at 25°C and 1 atm total pressure. *Geochim. Cosmochim. Acta.* 48: 2021-2035.

Busenberg, E. and Plummer, L.N. 1986. The solubility of  $\text{BaCO}_3$ (cr)(witherite) in  $\text{CO}_2$ - $\text{H}_2\text{O}$  solutions between 0 and 90°C, evaluation of the association constants of  $\text{BaHCO}_3^+$ (aq) and  $\text{BaCO}_3^0$ (aq) between 5 and 80°C, and a preliminary evaluation of the thermodynamic properties of  $\text{Ba}^{2+}$ (aq). *Geochim. Cosmochim. Acta.* 50:2225-2234.  
Butler, J.N. 1964. *Ionic Equilibrium*. Addison-Wesley, Reading, MA., 400pp.

Cameron, F.K., Bell, I.M., and Robinson, W.Q. 1907. The solubility of certain salt present in alkali soils. *J. Phys. Chem.* 11:396-420.

CODATA Task Group on Key Values for Thermodynamics. 1977. Recommended key values for thermodynamics, 1976. *J. Chem. Thermodyn.* 9:705-706.

Debye, P. and Huckel, E. 1923. On the theory of electrolytes. *Phys. Z.* 24:185-208, 305-325.

Dutton, S.P. 1982. Depositional history and reservoir quality of granite wash. *Texas Bur. Econ. Geol. Circ.* 82-7, 87-90.

Fisher, R.S. and Kreitler, C.W. 1985. *Geochemistry of deep-basin brines, Palo Duro basin, Texas*. OF-WTWI-1985-44. Texas Bur. Econ Geol.

Frear, G.L. and Johnson, J. 1929. The solubility of calcium carbonate (calcite) in certain aqueous solutions at 25°C. *J. Amer. Chem. Soc.* 51:2082-2093.

Fukui, L.M. and Dayvault, R.D. 1985. Summary of petrographic data for deep aquifer samples, Palo Duro basin, Texas. Subcontract E511-13700 to Battelle Proj. Mgmt. Div., Office of Nuclear Waste Isolation under U.S. Dept. of Energy Contracts DE-AC06-76RL01830 and DE-AC02-83CH10140, 113 pp.

Garrels, R.M. and Christ, C.L. 1965. *Solutions, Minerals and Equilibria*. Freeman and Cooper, San Francisco, CA. 450pp.

- Goldberg, R.N. and Nuttal, R.L. 1978. Evaluated Activity and Osmotic Coefficients for Aqueous Solutions: The Alkaline Earth Metal Halides. *J. Phy. Chem. Ref. Data.* 7(1):263-310.
- Hansson, I. 1973. A new set of acidity constants for carbonic acid and boric acid in seawater. *Deep Sea Res.* 20:461-478.
- Harvie, C.E. 1981. Theoretical Investigations in Geochemistry and Atom Surface Scattering. PhD dissertation, University of Calif., San Diego, CA.
- Harvie, C.E., Moller, N. and Weare J.H. 1984. The prediction of mineral solubilities in natural waters: The Na-K-Mg-Ca-H-Cl-SO<sub>4</sub>-OH-HCO<sub>3</sub>-CO<sub>3</sub>-CO<sub>2</sub>-H<sub>2</sub>O system to high ionic strengths at 25°C. *Geochim. Cosmochim. Acta.* 48:723-751.
- Hubbard N.(1984) Personal communication, Battelle Columbus.
- Jenne, E.A., Ball, J.W., Buchard, J.M., Vivit, D.V. and Barks, J.H. 1980. Geochemical modeling of Apparent solubility controls of Ba, Zn, Cd, Pb and F in waters of the Missouri Tri-state mining area. *in* Trace Substances in Environmental Health-IV, (ed. D.D. Hemphill), Univ. Missouri, Columbia, MO., pp. 353-361.
- Kline, W.D. 1929. The solubility of magnesium carbonate (nesquehonite) in water at 25°C and pressures of carbon dioxide up to 1 atm. *J. Amer. Chem. Soc.* 51:2093-2097.
- Langmuir, D. 1965. Stability of carbonates in the system MgO-CO<sub>2</sub>-H<sub>2</sub>O. *J. Geol.* 73:730-754.
- Langmuir, D. 1978. Uranium solution-mineral equilibria at low temperatures with applications to sedimentary ore deposits. *Geochim. Cosmochim. Acta.* 42:547-569.
- Langmuir, D. 1984. Physical and chemical characteristics of carbonate water. *in* Guide to the hydrology of carbonate rocks., UNESCO, 343p.
- Langmuir, D. and Herman, J.S. 1980. The mobility of thorium in natural waters at low temperatures. *Geochim. Cosmochim. Acta.* 44:1753-1766.
- Langmuir, D. and Melchior, D. 1985. The geochemistry of Ca, Sr, Ba and Ra sulfates in some deep brines from the Palo Duro basin, Texas. *Geochim. Cosmochim. Acta.* 49:2423-2432.

Laul, J.C., Perkins, R.W. and Hubbard, N. 1983. The behavior of natural radionuclides in brine groundwaters. Abstract, 96th Annual meeting Geological Society of America, Indianapolis, IN.

Lemire, R.J. and Tremaine P.R. 1980. Uranium and plutonium equilibria in aqueous solutions to 200°C., J. Chem. Eng. Data. 25:361-370.

Lown, D.A., Thirsk, H.R. and Wynne-Jones, L. 1968. Effect of pressure on ionization equilibria in water at 25°C. Trans. Faraday Soc. 64:2073-2080.

MacDonald, R.W. and North, N.A. 1974. The effect of pressure on the solubility of  $\text{CaCO}_3$ ,  $\text{CaF}_2$  and  $\text{SrSO}_4$  in water. Can. J. Chem. 52:3181-3186.

Marshall, W.L. and Chen, C.A. 1982. Amorphous silica solubilities V. Predictions of solubility behavior in aqueous mixed electrolyte solutions to 300°C. Geochim. Cosmochim. Acta. 46:289-291.

Martell, A.E. and Smith, R. M. 1977. Critical Stability Constants, Volume 3: Other Organic Ligands, Plenum Press, New York, NY. 495pp.

Means, J. (1986) Personal communication, Battelle Columbus.

Melchior, D.C. 1984. The Application of Ion-Interaction Theory of Electrolytes to the Solubilities of Copper and of some Alkaline-Earth Sulfates in Brines. PhD dissertation, Col. School of Mines, Golden, CO.

Millero, F.J. 1982. The effect of pressure on the solubility of minerals in water and seawater. Geochim. Cosmochim. Acta. 46:11-22.

Millero, F.J. 1983. The estimation of the  $\text{pK}_{\text{HA}}^*$  of acids in seawater using the Pitzer equations. Geochim. Cosmochim. Acta. 47:2121-2131.

Millero, F.J., Milne, P.J. and Thurmond, V.L. 1984. The solubility of calcite, strontianite and witherite in NaCl solutions at 25°C. Geochim. Cosmochim. Acta. 48:1141-1144.

Ming, D.W. 1981. Chemical and crystalline properties of minerals in the  $\text{MgO-CO}_2\text{-H}_2\text{O}$  system. PhD dissertation, CSU, Fort Collins, CO.

Mitchell, A.E. 1923. Studies on the dolomite system, part II. J. Chem. Soc. 123:1887-1904.

Monnin, C. and Schott, J. 1984. Determination of the solubility products of sodium carbonate minerals and application to trona deposition in Lake Magadi (Kenya). Geochim. Cosmochim. Acta. 48:571-581

Mucci, A. and Morse, J.W. 1983. The incorporation of  $Mg^{2+}$  and  $Sr^{2+}$  into calcite overgrowths: influences of growth rate and solution composition. Geochim. Cosmochim. Acta. 47: 217-233.

Nordstrom, D.K. and Ball, J.W. 1984. Chemical models, computer programs and metal complexation in natural waters. in Complexation of Trace Metals in Natural Waters, Kramer, C.J. M. and Duinker, J.C., ed. Martinus Nijhoff/ Dr. W. Junk Pub., 150-165.

Nordstrom, D.K. and Munoz, J.L. 1986. Geochemical Thermodynamics, Blackwell Sci. Pub., New York, N.Y., 477p.

Parks, G. 1984. Unpublished data. Stanford Univ.

Peiper, J.C. and Pitzer, K.S. 1982. Thermodynamics of aqueous carbonate solutions including mixtures of sodium carbonate, bicarbonate and chloride. J. Chem Thermodyn. 14:613-638.

Pitzer, K.S. 1977. Electrolyte Theory- improvements since Debye-Huckel. Acc. Chem. Res. 10:371-377.

Pitzer, K.S. 1979. Theory: Ion interaction approach. in Activity Coefficients in Electrolyte Solutions, (ed. R. M. Pytkowicz), Vol. 1, CRC Press, 159-209.

Pitzer, K.S. 1987. A thermodynamic model for aqueous solutions of liquid-like density. in. Reviews in Mineralogy, Vol. 17. Thermodynamic modeling of geological materials. Minerals, fluids and melts. (ed. I.S.E. Carmichael and H.P. Eugster). Mineral. Soc. Amer., 97-142.

Pitzer, K.S. and Peiper, J.C. 1980. Activity coefficient of aqueous  $NaHCO_3$ . J. Phys. Chem. 84:2396-2398.

Plummer, L.N. and Busenberg, E. 1982. The solubilities of calcite, aragonite and vaterite in  $\text{CO}_2\text{-H}_2\text{O}$  solutions between 0 and  $90^\circ\text{C}$ , an evaluation of the aqueous model for the system  $\text{CaCO}_3\text{-CO}_2\text{-H}_2\text{O}$ . *Geochim. Cosmochim. Acta.* 46:1011-1037.

Reardon, E.J. 1974. Thermodynamic properties of some sulfate, carbonate and bicarbonate ion pairs. PhD dissertation, The Pennsylvania State Univ., PA.

Reardon, E.J. and Armstrong, D.K. 1987. Celestite ( $\text{SrSO}_4$ ) solubility in water, seawater and NaCl solution. *Geochim. Cosmochim. Acta.* 51:63-72.

Reardon, E.J. and Langmuir, D. 1974. Thermodynamic properties of the ion pairs  $\text{MgCO}_3$  and  $\text{CaCO}_3$  from 10 to  $50^\circ\text{C}$ . *Amer. J. Sci.* 274:599-612.

Robie, R.A. and Hemingway, B.S. 1973. The enthalpies of formation of nesquehonite and hydromagnesite. *J. Res. U.S. Geol. Survey.* 5:543-547.

Robins, R.G. 1967. Hydrothermal precipitation in solutions of thorium nitrate, ferric nitrate and aluminum nitrate. *J. Inorg. Nucl. Chem.* 29:431-435.

Robinson, R.A. 1955. The osmotic and activity coefficients of aqueous solution of thorium chloride at  $25^\circ\text{C}$ . *J. Amer. Chem. Soc.* 77:6200.

Robinson, R.A. and Stokes, R.H. 1959. *Electrolyte Solutions*, (2nd Ed.) Butterworths Sci. Pub., London, 559 pp.

Rogers, P.Z.K. 1981. *Thermodynamics of Geothermal Fluids*, PhD. Thesis, Univ. of California, Berkely, CA.

Roy, R.N., Gibbons, J.J., Wood, M.D., Peiper, J.C. and Pitzer, K.S. 1983. The first ionization of carbonic acid in solutions of potassium chloride including the activity coefficients of potassium bicarbonate. *J. Chem. Thermodyn.* 15:37-47.

Schott, J. and Dandurand, J.L. 1975. Stability of natural carbonates. New values for the free energies of formation of phases in the  $\text{MgO-CO}_2\text{-H}_2\text{O}$  and  $\text{CaO-MgO-CO}_2\text{-H}_2\text{O}$  systems. *C. R. Hebd. Seances Acad. Sci. Ser. C.* 280:1247-1250.

Shternina, E.B. and Frolova, E.V. 1952. The solubility of calcite in the presence of  $\text{CO}_2$  and  $\text{NaCl}$ . Iz. Sek, Fiz. Khim. Anal. Inst. Ob. Neorg. Khim. Akad. Nauk SSSR. 21:271-287.

Shternina, E.B. and Frolova, E.V. 1962. Extraction of ballast carbonates from Kara-Tau Phosphorite ore. Zh. Prikl. Khim. 35:751-756.

Skoog, D.A. and West, D.M. 1974. Analytical Chemistry, an Introduction., Holt, Rinehart, and Winston., New York, NY., 430 pp.

Smith, D.A., Akhter, S. and Kreitler, C.W. 1985. Ground water hydraulics of the deep basin aquifer system, Palo Duro basin, Texas panhandle. Texas Bur. Econ. Geol. report OF-WTWI-1985-16, 67p.

Smith, R.M. and Martell, A.E. 1976. Critical Stability Constants. Vol. 4, Inorganic Complexes. Plenum Press, New York, N.Y., 700pp.

Sverjensky, D.A. 1984. Prediction of Gibbs free energies of calcite-type carbonates and the equilibrium distribution of trace elements between carbonate and aqueous solutions. Geochim. Cosmochim. Acta. 48:1127-1134.

Tredafelov, D., Markov, L. and Balarev, Kh. 1981. Phase equilibria in the  $\text{MgCO}_3$ - $\text{MgSO}_4$ - $\text{H}_2\text{O}$  and  $\text{MgCO}_3$ - $\text{MgCl}_2$ - $\text{H}_2\text{O}$  systems at 25 C in a  $\text{CO}_2$  atmosphere. Russ. J. Inorg. Chem. 26:907-909.

Truesdell, A.H. and Jones, B.F. 1974. WATEQ, a computer program for calculating chemical equilibria of natural waters. J. Res. U.S. Geol. Survey. 2:23-248.

Wagman, D.D., Evans, W.H., Parker, V.B., Schumm, R.H., Halow, I., Bailey, S.M., Churney, K.L. and Nuttall, R.L. 1982. The NBS Tables of Chemical Thermodynamic Properties. Selected values for inorganic and  $\text{C}_1$  and  $\text{C}_2$  organic substances in SI units. J. Phys. Chem. Ref. Data 11, Suppl. No. 2, 392pp.

Weare, J.H. 1987. Models of mineral solubility in concentrated brines with application to field observations. in. Reviews in Mineralogy, Vol 17. Thermodynamic modeling of geological materials. Minerals, fluids and melts. (ed. I.S.E. Carmichael and H.P. Eugster). Mineral. Soc. Amer., 143-160.

Zaikowski, A., Kosanke, B.J. and Hubbard, N. 1987. Noble gas composition of deep brines from the Palo Duro Basin, Texas. *Geochim. Cosmochim. Acta.* 51:73-84.

APPENDIX IPitzer ion-interaction equations

The Pitzer ion-interaction approach to computing ion activity coefficients is based on a set of theoretically and empirically derived equations which account for both long-range and short-range electrostatic interactions between ions. The basic equation is a virial coefficient expansion of a modified Debye-Huckel expression. Binary interaction parameters ( $\beta^0$ ,  $\beta^1$ ,  $\beta^2$  and  $C^0$ ) account for interactions of two ions of opposite sign. The magnitude of  $\beta^2$  for a particular cation-anion pair is directly related to the strength of association between the two ions. Higher-order binary ( $\phi_{ij}$ ) and ternary ( $\psi_{ijk}$ ) parameters account for the effects of mixing unsymmetrical electrolytes (Pitzer, 1987). The general form of the Pitzer equation for computing the mean activity coefficient of a salt (MX) is:

$$\begin{aligned} \ln \gamma_{MX} &= |z_M z_X| F^2 + (2\nu_M/\nu) \sum_a m_a [B_{Ma} + (\sum m_z) C_{Ma} \\ &+ (\nu_X/\nu_M) \theta_{Xa}] + (2\nu_X/\nu) \sum_c m_c [B_{cX} + (\sum m_z) C_{cX} \\ &+ (\nu_M/\nu_X) \theta_{Mc}] + \sum_c \sum_a m_c m_a \{ |z_M z_X| B'_{ca} \\ &+ \nu^{-1} [2\nu_M z_M C_{ca} + \nu_M \psi_{Mca} + \nu_X \psi_{caX}] \} \\ &+ \frac{1}{2} \sum_c \sum_{c'} m_c m_{c'} [(\nu_X/\nu) \psi_{cc'X} \\ &+ |z_M z_X| \theta'_{cc'}] + \frac{1}{2} \sum_a \sum_{a'} m_a m_{a'} [(\nu_M/\nu) \psi_{Maa'} \\ &+ |z_M z_X| \theta'_{aa'}] \end{aligned}$$

where  $f^Y = -A_\phi \left( \frac{I^{1/2}}{1 + 1.2I^{1/2}} + \frac{2}{1.2} \ln(1 + 1.2I^{1/2}) \right)$ ,

$A_\phi = 1/3 A_\gamma$ , the Debye-Hückel slope,  $I = 1/2 \sum_i m_i z_i^2$ ,

$$B_{MX} = \beta_{MX}^0 + \frac{2\beta_{MX}^1}{\alpha^2 I} [1 - (1 + \alpha_1 I^{1/2}) \exp(-\alpha_1 I^{1/2})] \\ + \frac{2\beta_{MX}^2}{\alpha^2 I} [1 - (1 + \alpha_2 I^{1/2}) \exp(-\alpha_2 I^{1/2})]$$

and  $C_{MX} = C_{MX}^\phi / 2 |z_M z_X|^{1/2}$

The terms  $v_M$  and  $v_X$  are the number of cations (M) and anions (X) in the neutral salt while  $v$  is the sum of  $v_M$  and  $v_X$ .

The charge on the cation and anion are  $z_M$  and  $z_X$  respectively. The constants  $\alpha_1$  and  $\alpha_2$  were derived empirically by Pitzer (1979). For 2-2 electrolytes,  $\alpha_1 = 1.4$  and  $\alpha_2 = 12.0$ . For all other electrolytes  $\alpha_1 = 2.0$  and  $\alpha_2 = 0$ . The terms  $B'$  and  $\phi'$  are the derivatives of  $B_{MX}$  and  $\phi_{ij}$  with respect to ionic strength.

The terms  $\phi_{ij}$  and  $\psi_{ijk}$  are required to model ion activities at high ionic strengths.  $\phi_{ij}$  accounts for interactions between two unlike ions of the same sign.  $\psi_{ijk}$  accounts for ternary interactions between two unlike ions of the same sign and one oppositely charged ion.